## Supporting Information

# Selective Separation of Methylfuran and Dimethylfuran by Nonporous Adaptive Crystals of Pillararenes

Yitao Wu,[a] Jiong Zhou,[a] Errui Li,[a] Mengbin Wang,[a] Kecheng Jie,[a] Huangtianzhi Zhu*,[a] and Feihe Huang*,[a,b]

[a] *State Key Laboratory of Chemical Engineering, Center for Chemistry of High-Performance & Novel Materials, Department of Chemistry, Zhejiang University, Hangzhou, 310027, P. R. China*

*Fax and Tel: +86-571-8795-3189; Email address: htzzhu@zju.edu.cn fhuang@zju.edu.cn*

[b] *Green Catalysis Center and College of Chemistry, Zhengzhou University, Zhengzhou 450001, P. R. China*

## Table of Content (48 pages)

*1. Materials*

All the starting materials including 2-methylfuran (**MeF**), 2,5-dimethylfuran (**DMeF**) and 2-methyltetrahydrofuran (**MeTHF**) were purchased and used as received. Pillar[*n*]arenes (**EtP5**, **EtP6**, **BrP5**, **BrP6**) were synthesized as described previously.[S1−S3] Activated crystalline **EtP5**, **EtP6**, **BrP5** and **BrP6** were referred to as **EtP5***α*, **EtP6***β*, **BrP5***α* and **BrP6***β* respectively. **EtP5***α*, **EtP6***β*, **BrP5***α* and **BrP6***β* were prepared according to reported procedures.[S4] All the mixtures were *v*:*v* = 1:1, except specifically marked mixtures.

**Table S1**. Physical properties of **MeF** and **DMeF**.[S5]

| Substance | Melting point (°C) | Boiling point (°C) | Saturated Vapor Pressure at 298 K (kPa) |
|---|---|---|---|
| **MeF** | –91.2 | 63.9 | 23.0 |
| **DMeF** | –62.8 | 96.0 | uncertain |

*2. Methods*

*2.1. Powder X-Ray Diffraction*

PXRD data were collected on a Rigaku Ultimate-IV X-Ray diffractometer operating at 40 kV/30 mA using the Cu K*α* line (*λ* = 1.5418 Å). Data were measured over the range 5–45° in 5°/min steps over 8 min.

*2.2. Thermogravimetric Analysis*

TGA analysis was carried out using a Q5000IR analyzer (TA Instruments) with an automated vertical overhead thermobalance. The samples were heated at 10 °C/min using $N_2$ as the protective gas.

*2.3. Single Crystal Growth*

Single crystals of guest-loaded **EtP5**, **EtP6**, **BrP5** or **BrP6** were grown by volatilization: 5.00 mg of dry **EtP5**, **EtP6**, **BrP5** or **BrP6** powder were put in a small vial where 1.00 mL of guest was added and the vial was heated until all the powder was dissolved. The light yellow crystals were got by volatilization for 2-15 days.

*2.4. Single Crystal X-ray Diffraction*

Single crystal X-ray diffraction data were collected on a Bruker D8 VENTURE CMOS X-ray diffractometer with graphite monochromatic Mo–K*α* radiation (*λ* = 0.71073 Å).

*2.5. Solution $^1$H NMR Spectroscopy*

$^{1}$H NMR spectra were recorded by using a Bruker Avance DMX 400 spectrometer and a Bruker Avance DMX 600 spectrometer.

*2.6. Gas Chromatography*

Gas chromatographic analysis: GC measurements were carried out using an Agilent 7890B instrument configured with an FID detector and a DB-624 column (30 m × 0.53 mm × 3.0 μm). Samples were analyzed using headspace injections and were performed by incubating the sample at 100 °C for 10 min followed by sampling 1.00 mL of the headspace. The total volume of the container is 10 mL; the mass of the solid in the container is about 10 mg; the total volume of the headspace is 1mL. The following GC method was used: the oven was programmed from 60 °C, and ramped in 5 °C $min^{-1}$ increments to 200 °C with 5 min hold; the total run time was 25 min; the injection temperature was 250 °C; the detector temperature was 280 °C with nitrogen, air, and make-up flow-rates of 35, 350, and 35 mL $min^{-1}$, respectively; helium (carrier gas) flow-rate was 3.0 mL $min^{-1}$. The samples were injected in the split mode (30:1).

*3. Crystallography Data*

**Table S2**. Experimental single crystal X-ray data for **EtP5** structures.

| | (**MeF**)$_2$@**EtP5** | (**DMeF**)$_2$@**EtP5** |
|---|---|---|
| Crystallization Solvent | 2-Methylfuran | 2,5-Dimethylfuran |
| Collection Temperature | 170 K | 170 K |
| Formula | $C_{60}H_{76}O_{11}$ | $C_{67}H_{86}O_{12}$ |
| *Mr* | 973.20 | 1083.35 |
| Crystal Size [mm] | 0.10 × 0.08 × 0.06 | 0.18 × 0.16 × 0.15 |
| Crystal System | triclinic | monoclinic |
| Space Group | P-1 | $P2_1/n$ |
| *a* [Å] | 13.1670(3) | 13.5823(3) |
| *b* [Å] | 14.7060(4) | 22.8453(6) |
| *c* [Å] | 30.3360(7) | 20.4508(5) |
| $\alpha$ [°] | 87.8340(8) | 90 |
| $\beta$ [°] | 86.7890(8) | 100.3730(10) |
| $\gamma$ [°] | 85.7650(9) | 90 |
| *V* [Å$^3$] | 5846.0(2) | 6242.0(3) |
| Z | 4 | 4 |
| $D_{calcd}$[g cm$^{-3}$] | 1.106 | 1.153 |
| $\mu$[mm$^{-1}$] | 0.386 | 0.401 |
| *F*(000) | 2096 | 2336 |
| Radiation | GaK$\alpha$ ($\lambda$ = 1.34139) | GaK$\alpha$ ($\lambda$ = 1.34139) |
| 2$\theta$ range [°] | 5.906–110.222 | 6.310–109.846 |
| Reflections collected | 21773 | 54766 |
| Independent reflections, $R_{int}$ | 21773, 0.1414 | 11814, 0.0435 |
| Data /restraints /parameters | 21773/333/1412 | 11814/0/726 |
| Final $R_1$ values ($I > 2\sigma(I)$) | 0.1337 | 0.0512 |
| Final $R_1$ values (all data) | 0.204 | 0.0608 |
| Final $wR(F_2)$ values (all data) | 0.3712 | 0.1398 |
| Goodness-of-fit on $F^2$ | 0.788 | 1.022 |
| Largest difference peak and hole [e.A$^{-3}$] | 0.69/–0.36 | 0.79/–0.42 |
| CCDC | 1975509 | 1975512 |

**Table S3**. Experimental single crystal X-ray data for **EtP6** structures.

| | **(MeF)$_2$@EtP6** | **DMeF@EtP6** |
|---|---|---|
| Crystallization Solvent | 2-Methylfuran | 2,5-Dimethylfuran |
| Collection Temperature | 170 K | 170 K |
| Formula | $C_{76}H_{95}O_{14}$ | $C_{78}H_{100}O_{14}$ |
| *Mr* | 1232.51 | 1261.57 |
| Crystal Size [mm] | 0.15 × 0.08 × 0.06 | 0.20 × 0.18 × 0.16 |
| Crystal System | monoclinic | triclinic |
| Space Group | C2/c | P-1 |
| *a* [Å] | 26.7857(15) | 12.8203(3) |
| *b* [Å] | 12.5558(7) | 12.9026(3) |
| *c* [Å] | 25.1482(14) | 12.9306(3) |
| $\alpha$ [°] | 90 | 61.2780(10) |
| $\beta$ [°] | 118.9570(3) | 73.3750(10) |
| $\gamma$ [°] | 90 | 78.5590(10) |
| *V* [Å$^3$] | 7400.4(7) | 1792.62(7) |
| Z | 4 | 1 |
| $D_{calcd}$[g cm$^{-3}$] | 1.106 | 1.169 |
| $\mu$[mm$^{-1}$] | 0.387 | 0.406 |
| *F*(000) | 2652.0 | 680.0 |
| Radiation | GaK$\alpha$ ($\lambda$ = 1.34139) | GaK$\alpha$ ($\lambda$ = 1.34139) |
| 2$\theta$ range [°] | 6.892–110.618 | 6.276–109.782 |
| Reflections collected | 35533 | 6612 |
| Independent reflections, $R_{int}$ | 6964, 0.0543 | 6612,0.0709 |
| Data /restraints /parameters | 6964/37/408 | 6612/0/424 |
| Final $R_1$ values ($I > 2\sigma(I)$) | 0.1408 | 0.0543 |
| Final $R_1$ values (all data) | 0.1509 | 0.0578 |
| Final $wR(F_2)$ values (all data) | 0.3525 | 0.1518 |
| Goodness-of-fit on $F^2$ | 0.922 | 1.037 |
| Largest difference peak and hole [e.A$^{-3}$] | 0.90/–0.43 | 0.31/–0.33 |
| CCDC | 1975510 | 1975511 |

**Table S4**. Experimental single crystal X-ray data for **BrP5** structures.

| | **(MeF)$_2$@BrP5** | **(DMeF)$_2$@BrP5** |
|---|---|---|
| Crystallization Solvent | 2-Methylfuran | 2,5-Dimethylfuran |
| Collection Temperature | 170 K | 293(2) K |
| Formula | $C_{60}H_{66}Br_{10}O_{11}$ | $C_{67}H_{76}Br_{10}O_{12}$ |
| *Mr* | 1762.22 | 1872.37 |
| Crystal Size [mm] | 0.08 × 0.06 × 0.06 | 0.15 × 0.08 × 0.06 |
| Crystal System | orthorhombic | monoclinic |
| Space Group | Pbcn | C2/c |
| *a* [Å] | 24.4691(9) | 28.6532(17) |
| *b* [Å] | 20.7774(8) | 12.3731(8) |
| *c* [Å] | 12.8545(5) | 44.2420(3) |
| $\alpha$ [°] | 90 | 90 |
| $\beta$ [°] | 90 | 108.8360(2) |
| $\gamma$ [°] | 90 | 90 |
| *V* [Å$^3$] | 6535.3(4) | 14845.0(17) |
| Z | 4 | 8 |
| $D_{calcd}$[g cm$^{-3}$] | 1.791 | 1.676 |
| $\mu$[mm$^{-1}$] | 5.539 | 6.883 |
| *F*(000) | 3456.0 | 7392.0 |
| Radiation | GaK$\alpha$ ($\lambda$ = 1.34139) | GaK$\alpha$ ($\lambda$ = 1.34139) |
| 2$\theta$ range [°] | 6.286–110.114 | 7.854–139.04 |
| Reflections collected | 62688 | 39826 |
| Independent reflections, $R_{int}$ | 6244, 0.1197 | 13447, 0.0616 |
| Data /restraints /parameters | 6244/57/394 | 13447/207/806 |
| Final $R_1$ values ($I > 2\sigma(I)$) | 0.0982 | 0.1619 |
| Final $R_1$ values (all data) | 0.1304 | 0.2183 |
| Final $wR(F_2)$ values (all data) | 0.3197 | 0.4225 |
| Goodness-of-fit on $F^2$ | 1.173 | 1.563 |
| Largest difference peak and hole [e.A$^{-3}$] | 2.33/–1.76 | 2.26/–2.08 |
| CCDC | 1975513 | 1975514 |

**Table S5**. Experimental single crystal X-ray data for **BrP6** structures.

| | **(MeF)$_2$@BrP6** | **DMeF@BrP6** |
|---|---|---|
| Crystallization Solvent | 2-Methylfuran | 2,5-Dimethylfuran |
| Collection Temperature | 170 K | 170 K |
| Formula | $C_{71}H_{78}Br_{12}O_{13}$ | $C_{78}H_{88}Br_{12}O_{14}$ |
| *Mr* | 2098.25 | 2208.40 |
| Crystal Size [mm] | 0.18 × 0.16 × 0.15 | 0.06 × 0.06 × 0.05 |
| Crystal System | triclinic | orthorhombic |
| Space Group | P-1 | Pbcn |
| *a* [Å] | 14.1746(4) | 13.8496(2) |
| *b* [Å] | 16.4665(6) | 23.9980(3) |
| *c* [Å] | 19.6666(6) | 25.2072(3) |
| $\alpha$ [°] | 79.1720(2) | 90 |
| $\beta$ [°] | 77.5990(2) | 90 |
| $\gamma$ [°] | 72.4790(2) | 90 |
| *V* [Å$^3$] | 4237.6(2) | 8377.93(19) |
| Z | 2 | 4 |
| $D_{calcd}$[g cm$^{-3}$] | 1.644 | 1.751 |
| $\mu$[mm$^{-1}$] | 4.954 | 5.041 |
| *F*(000) | 2056.0 | 4352.0 |
| Radiation | GaK$\alpha$ ($\lambda$ = 1.34139) | GaK$\alpha$ ($\lambda$ = 1.34139) |
| 2$\theta$ range [°] | 5.952–109.948 | 6.410–109.860 |
| Reflections collected | 44643 | 88933 |
| Independent reflections, $R_{int}$ | 16022, 0.0540 | 7963, 0.0420 |
| Data /restraints /parameters | 16022/149/957 | 7963/0/481 |
| Final $R_1$ values ($I > 2\sigma(I)$) | 0.1095 | 0.0391 |
| Final $R_1$ values (all data) | 0.1333 | 0.0421 |
| Final $wR(F_2)$ values (all data) | 0.2756 | 0.1041 |
| Goodness-of-fit on $F^2$ | 0.925 | 1.037 |
| Largest difference peak and hole [e.A$^{-3}$] | 2.67/–2.29 | 1.62/–1.21 |
| CCDC | 1975516 | 1975515 |

*4. Characterization of Activated Pillararene Crystals*

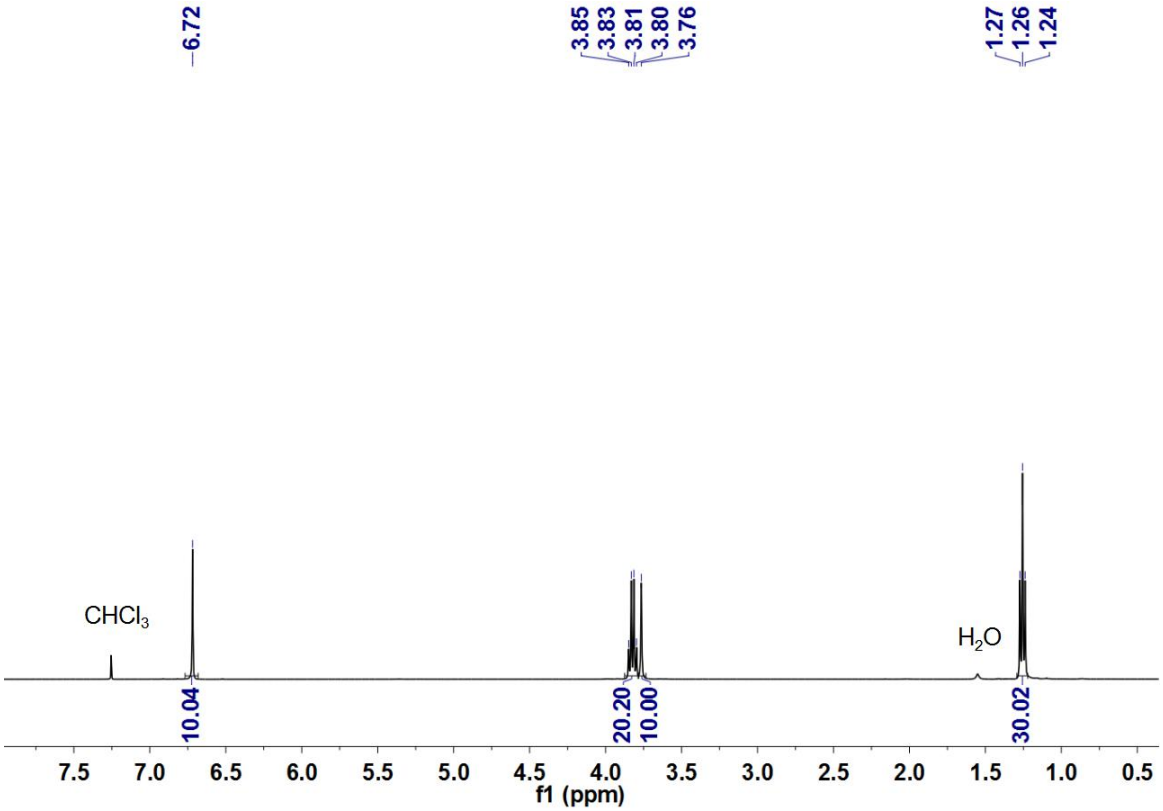


**Figure S1.** $^{1}$H NMR spectrum (600 MHz, chloroform-*d*, 298 K) of **EtP5***α*

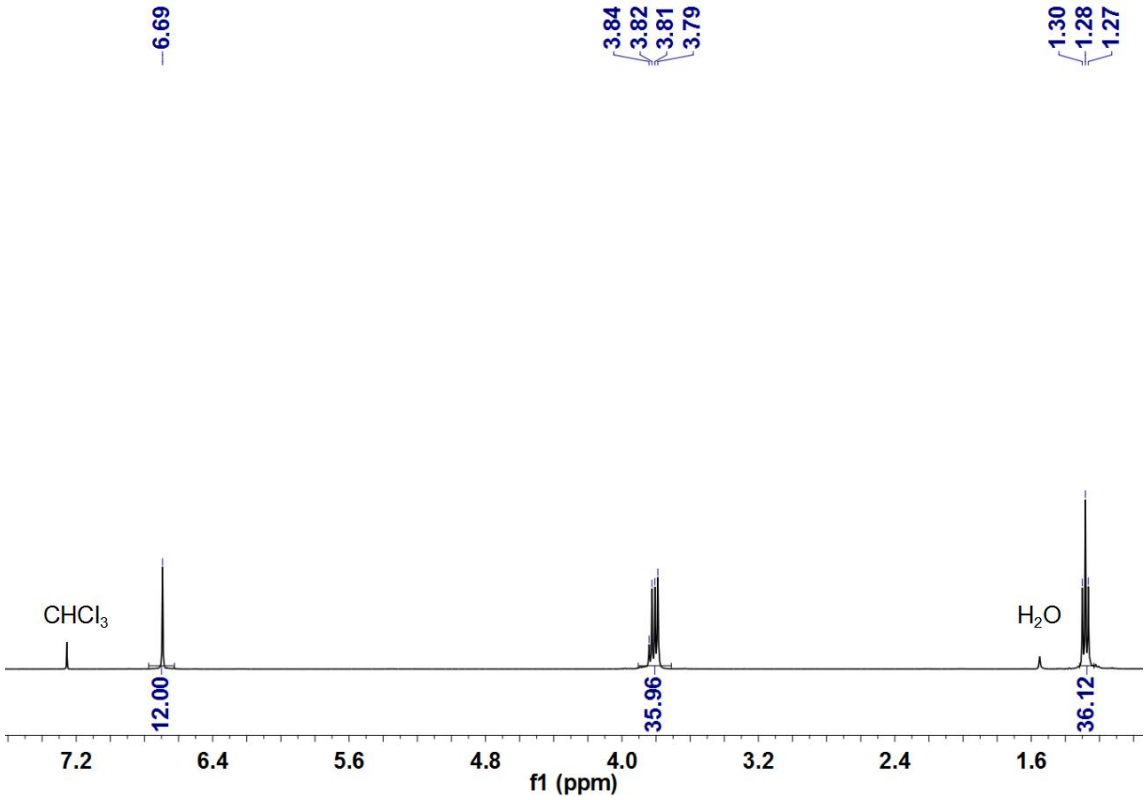


**Figure S2.** $^{1}$H NMR spectrum (600 MHz, chloroform-*d*, 298 K) of **EtP6***β*

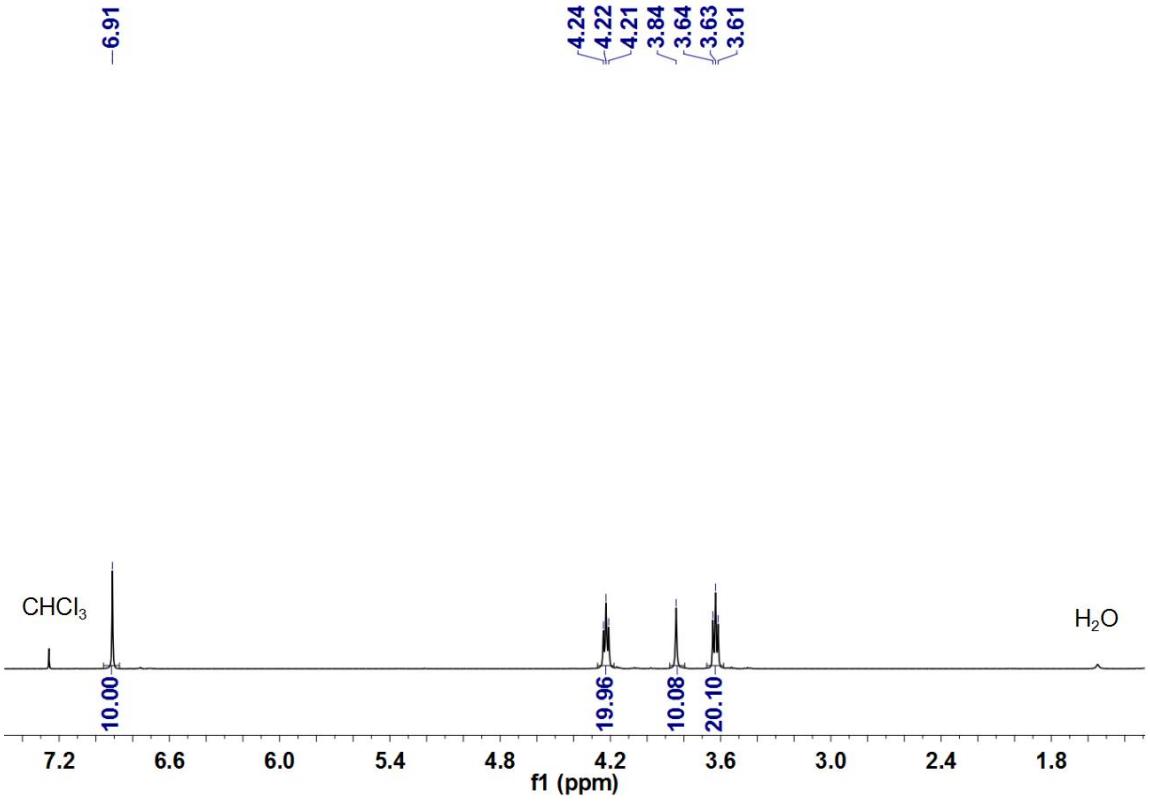


**Figure S3.** [1]H NMR spectrum (600 MHz, chloroform-*d*, 298 K) of **BrP5***α*

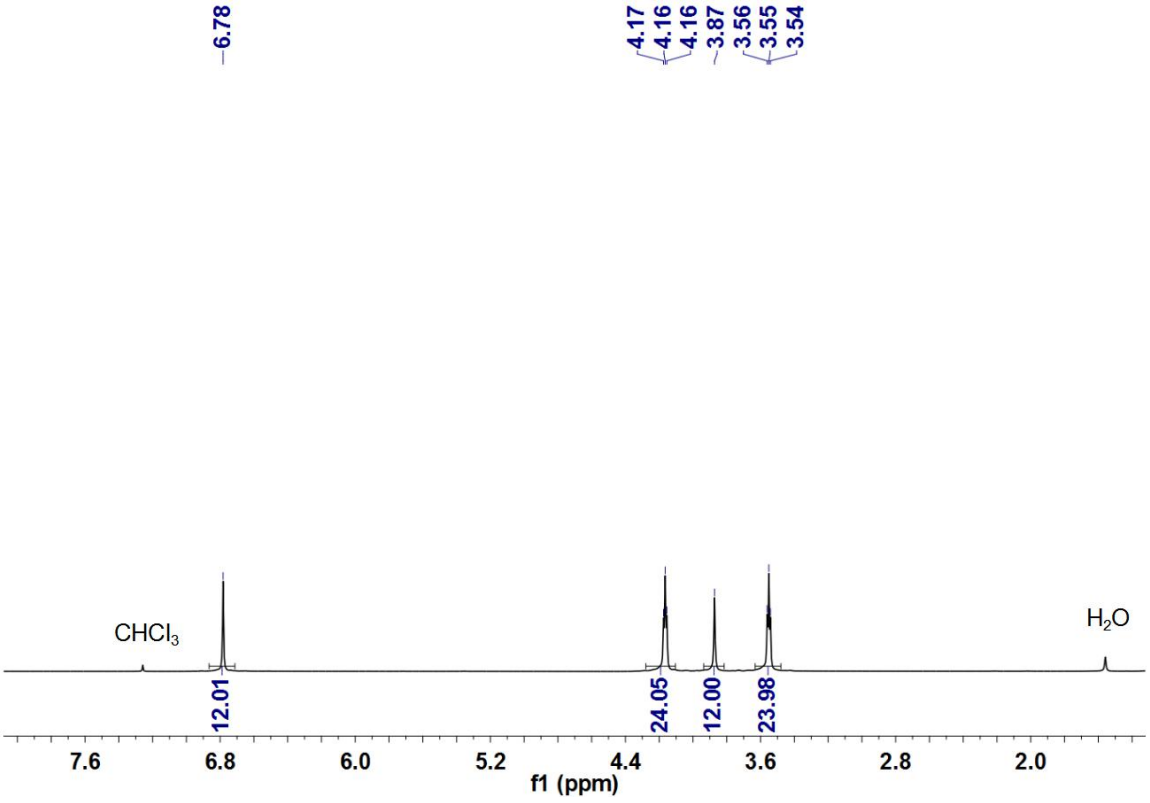


**Figure S4.** [1]H NMR spectrum (600 MHz, chloroform-*d*, 298 K) of **BrP6***β*

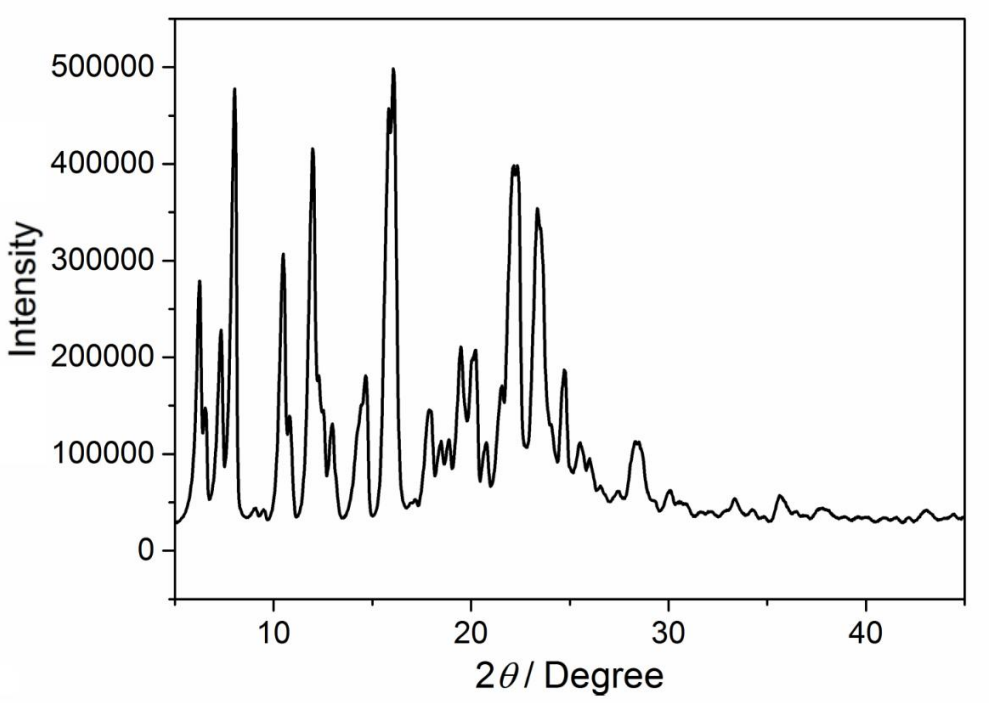


**Figure S5.** Powder X-ray diffraction pattern of **EtP5***α*

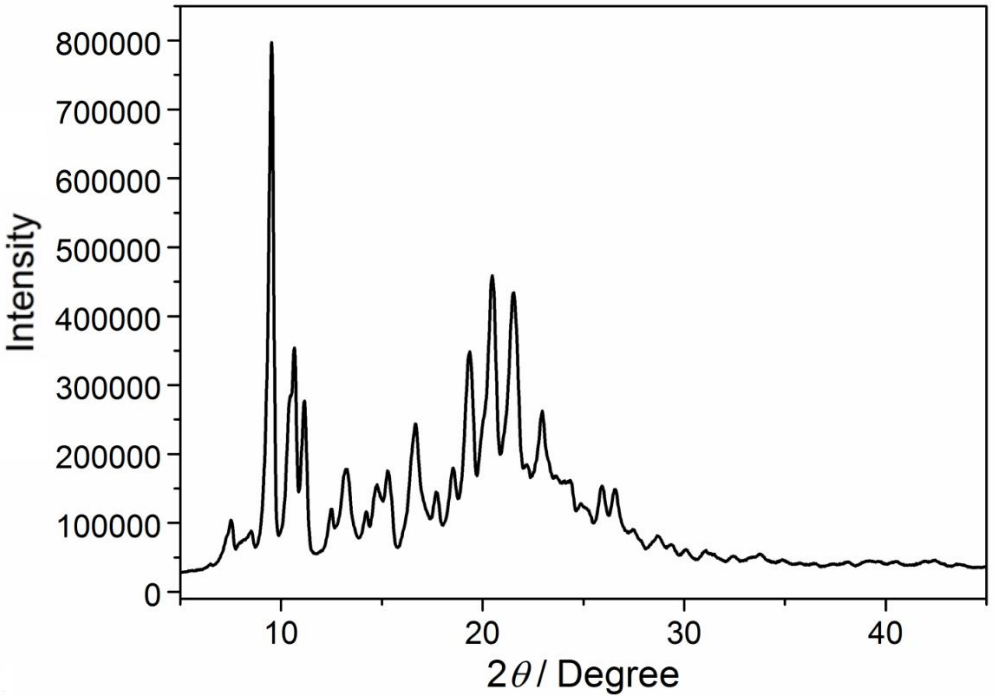


**Figure S6.** Powder X-ray diffraction pattern of **EtP6***β*

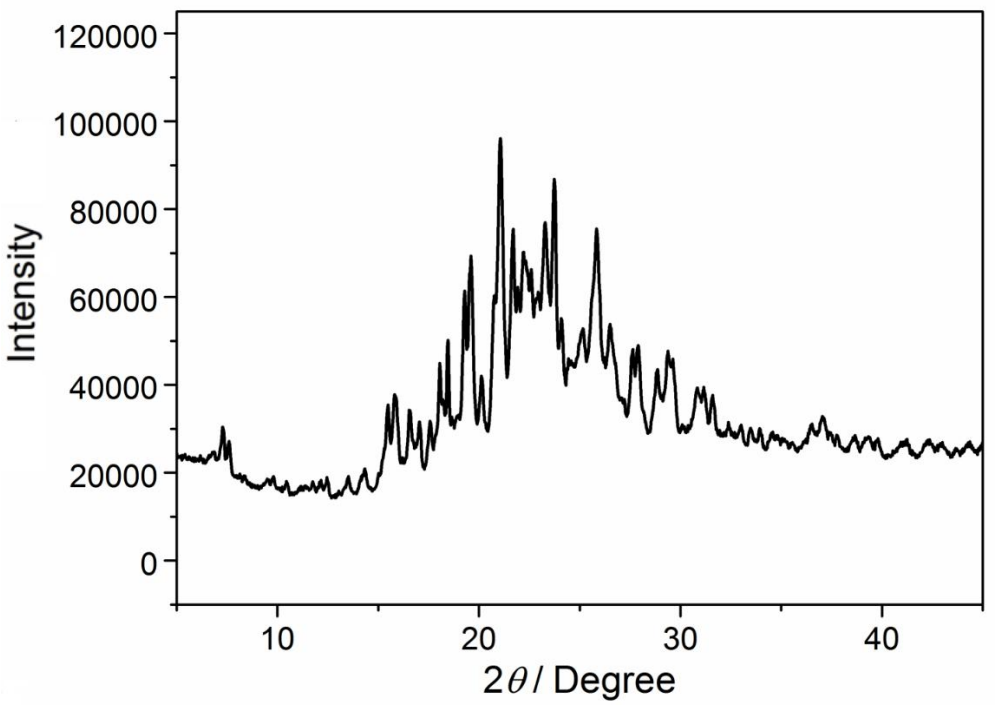


**Figure S7.** Powder X-ray diffraction pattern of **BrP5***α*

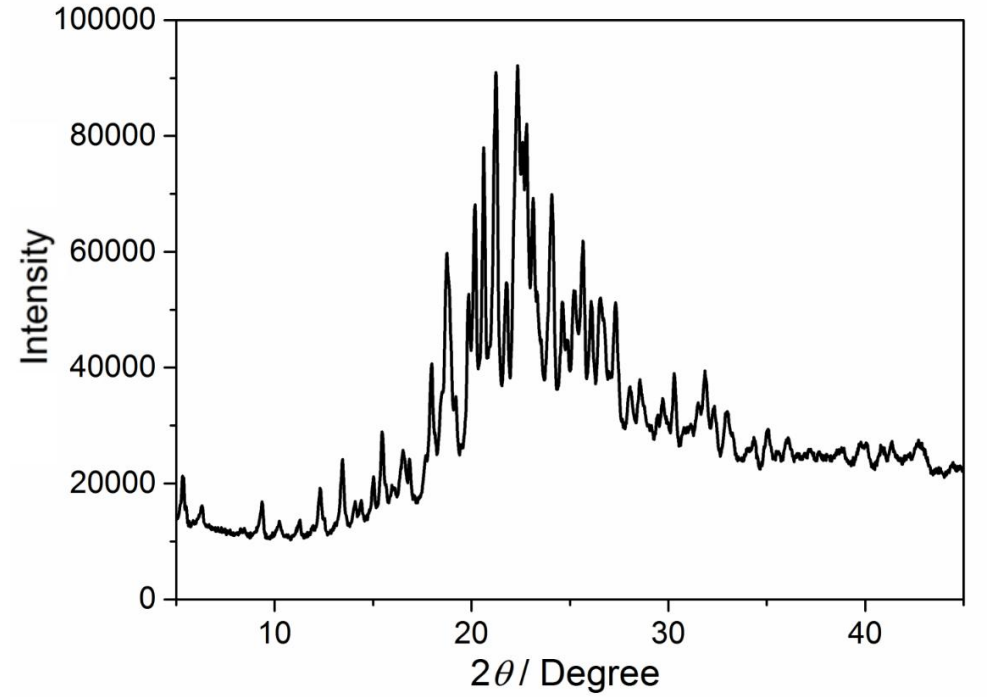


**Figure S8.** Powder X-ray diffraction pattern of **BrP6***β*

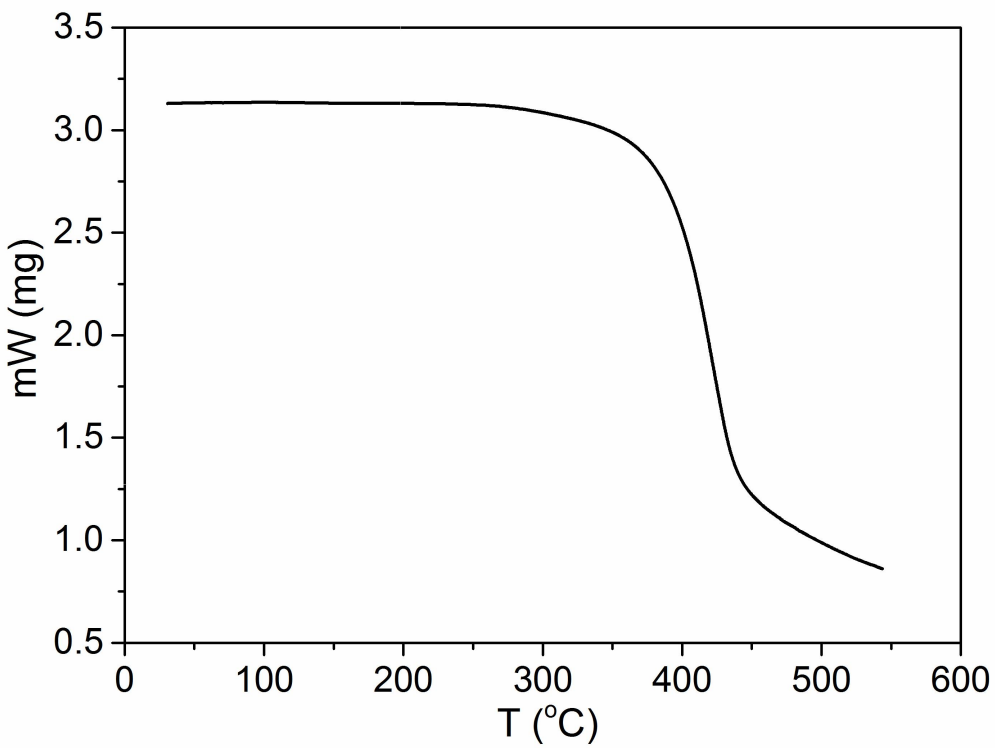


**Figure S9.** Thermogravimetric analysis of desolvated **EtP5***α*

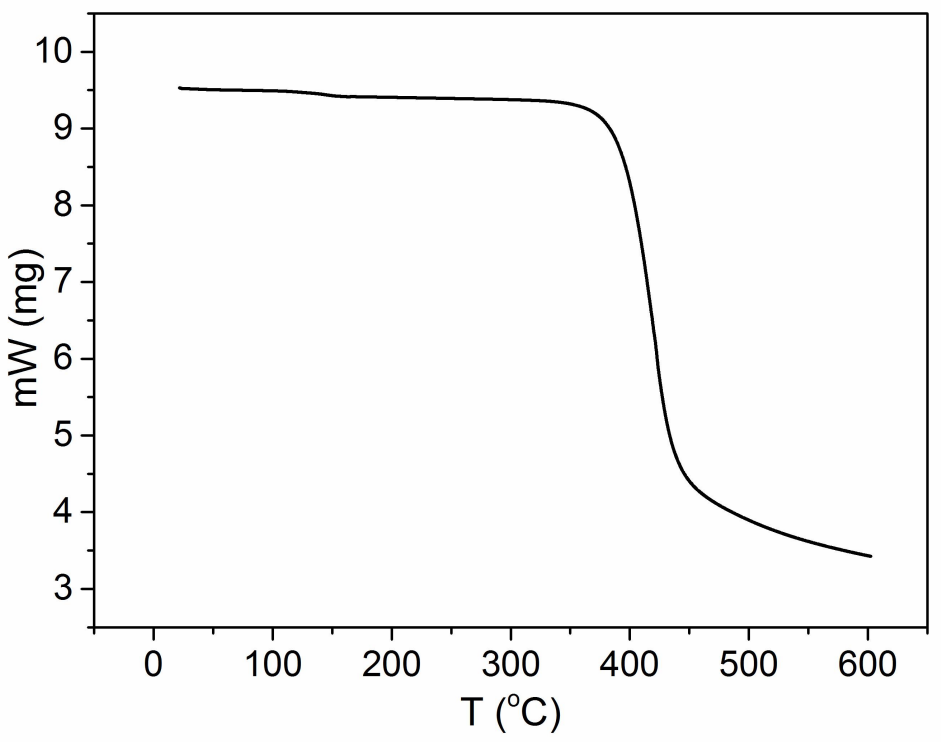


**Figure S10.** Thermogravimetric analysis of desolvated **EtP6***β*

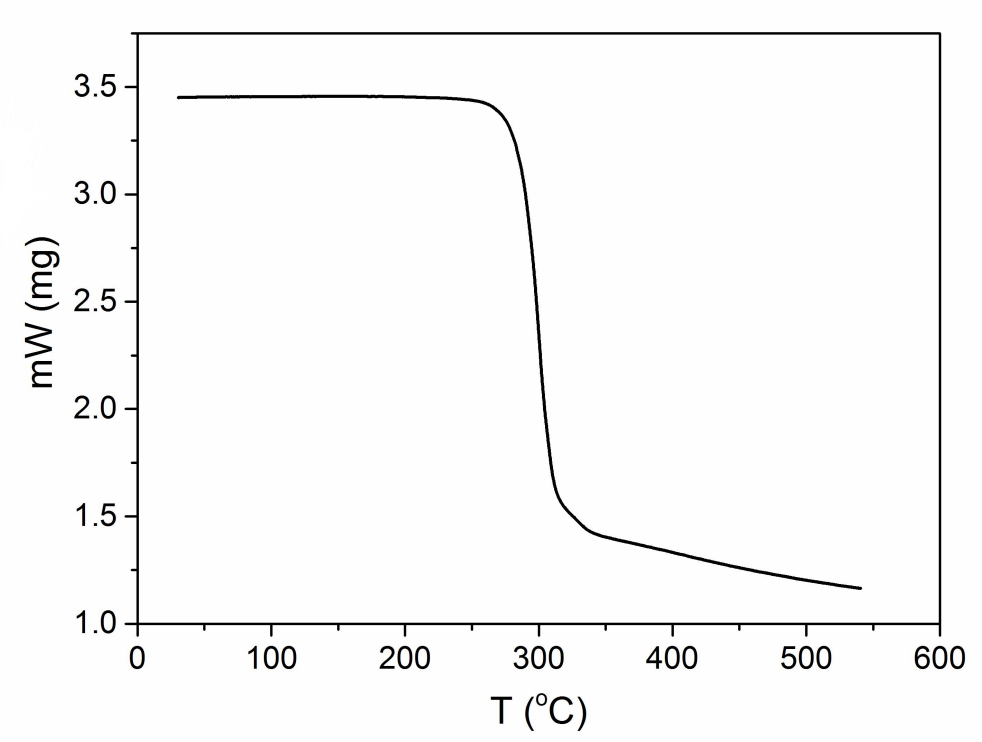


**Figure S11.** Thermogravimetric analysis of desolvated **BrP5***α*

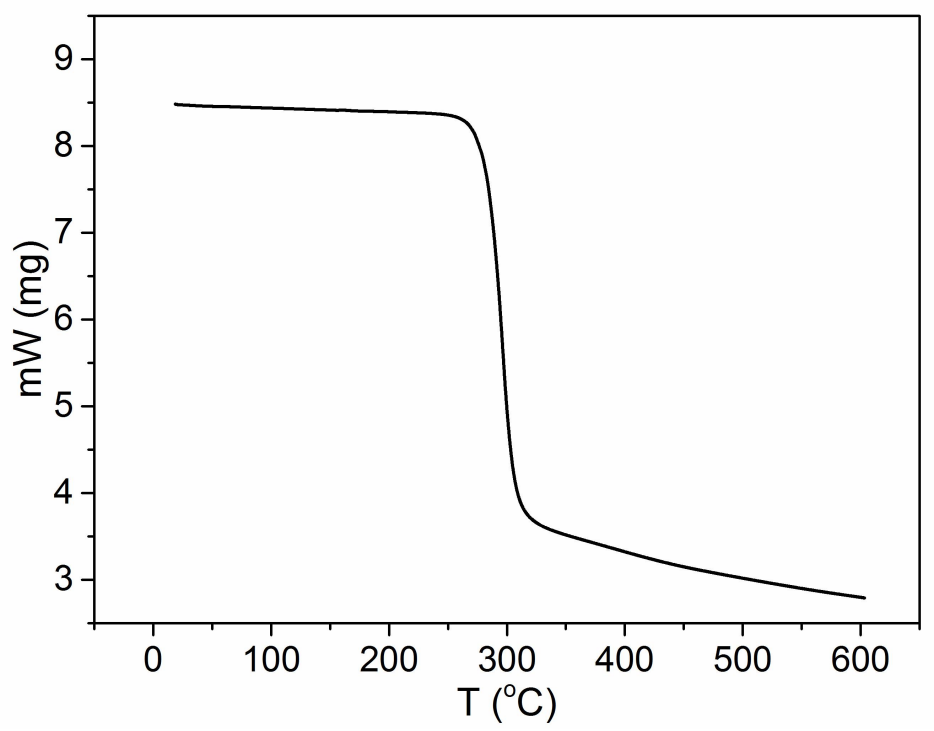


**Figure S12.** Thermogravimetric analysis of desolvated **BrP6***β*

*5. Vapor-Phase Adsorption Measurements*

*5.1. Single-Component **MeF** and **DMeF** Adsorption Experiments*

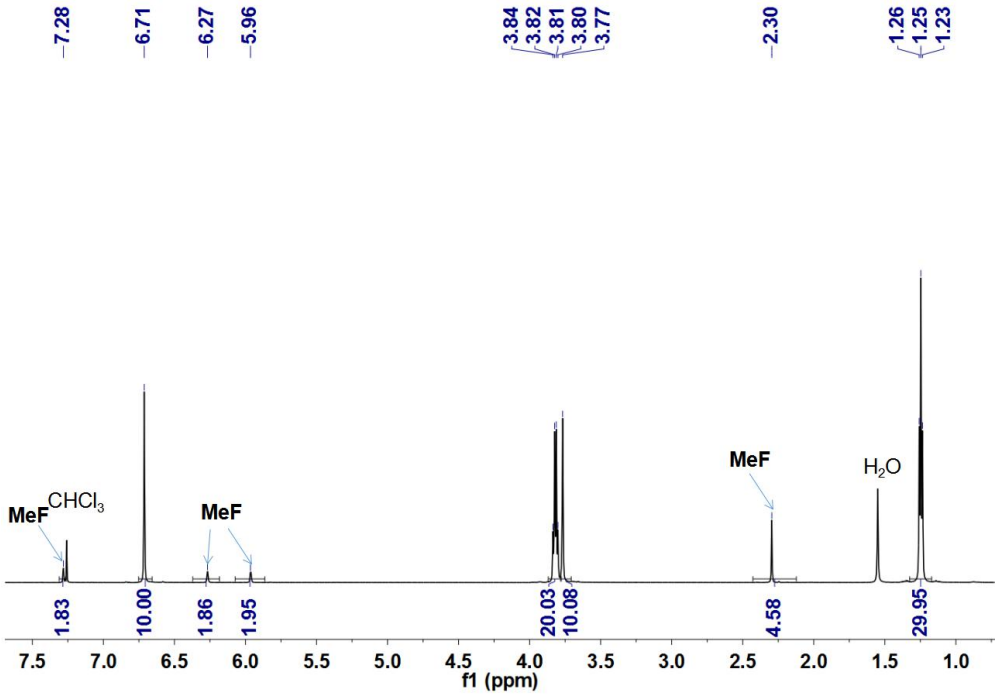


**Figure S13.** $^{1}$H NMR spectrum (600 MHz, chloroform-*d*, 298 K) of **EtP5***α* after adsorption of **MeF** vapor.

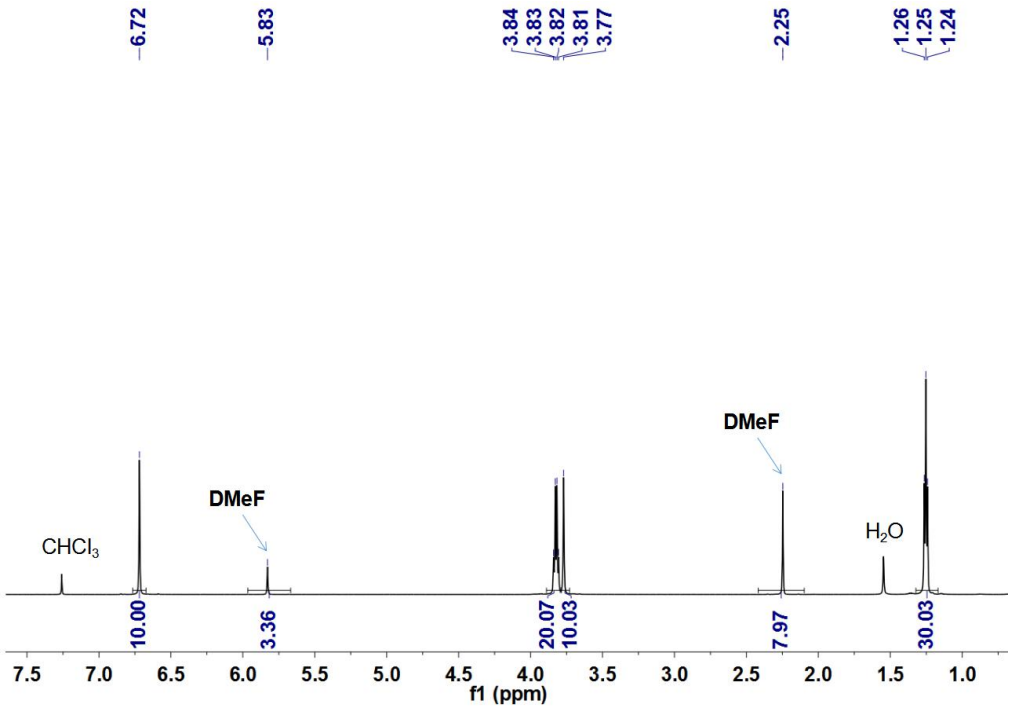


**Figure S14.** $^{1}$H NMR spectrum (600 MHz, chloroform-*d*, 298 K) of **EtP5***α* after adsorption of **DMeF** vapor.

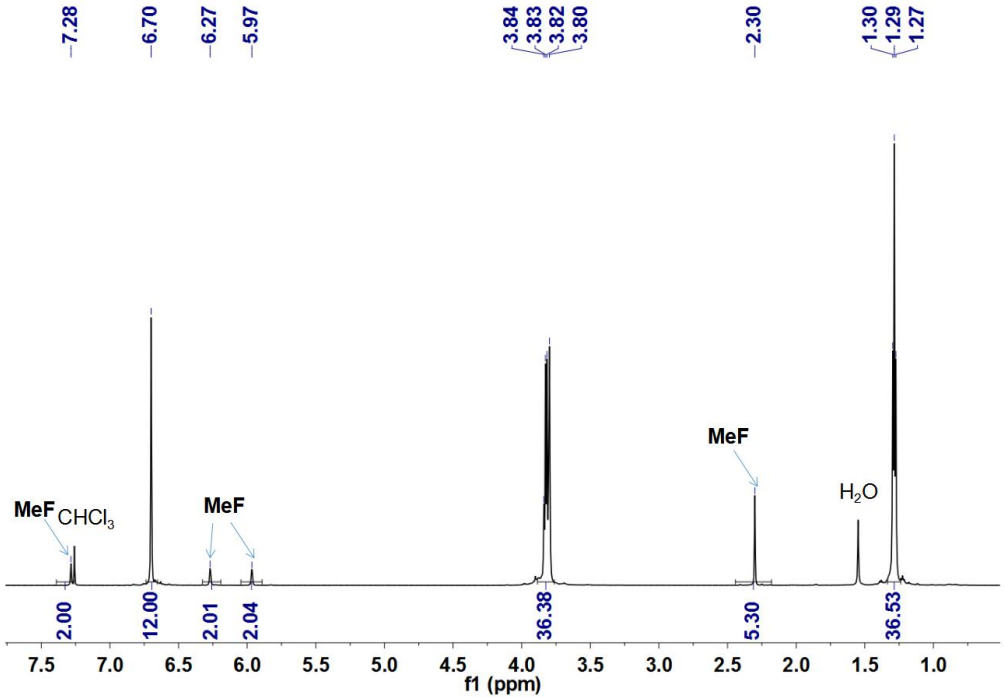


**Figure S15.** $^{1}$H NMR spectrum (600 MHz, chloroform-*d*, 298 K) of **EtP6*β*** after adsorption of **MeF** vapor.

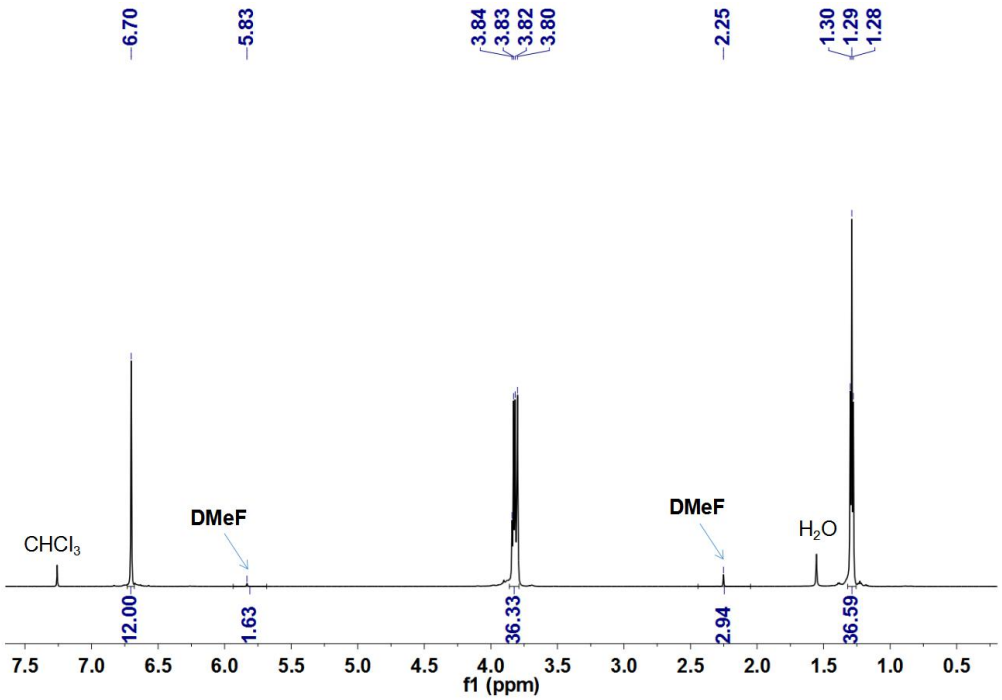


**Figure S16.** $^{1}$H NMR spectrum (600 MHz, chloroform-*d*, 298 K) of **EtP6*β*** after adsorption of **DMeF** vapor.

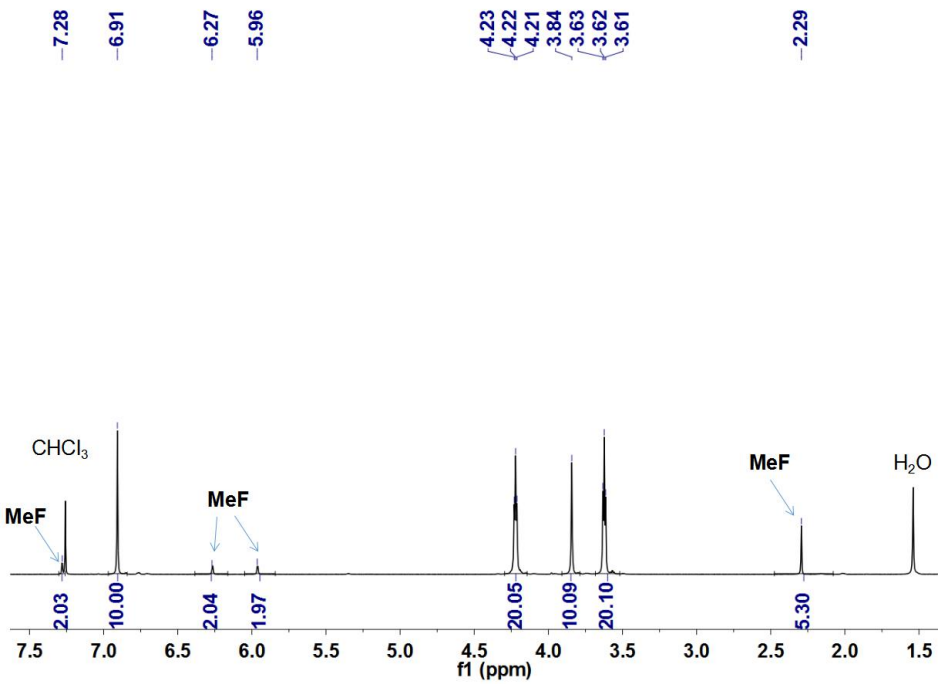


**Figure S17.** [1]H NMR spectrum (600 MHz, chloroform-*d*, 298 K) of **BrP5***α* after adsorption of **MeF** vapor.

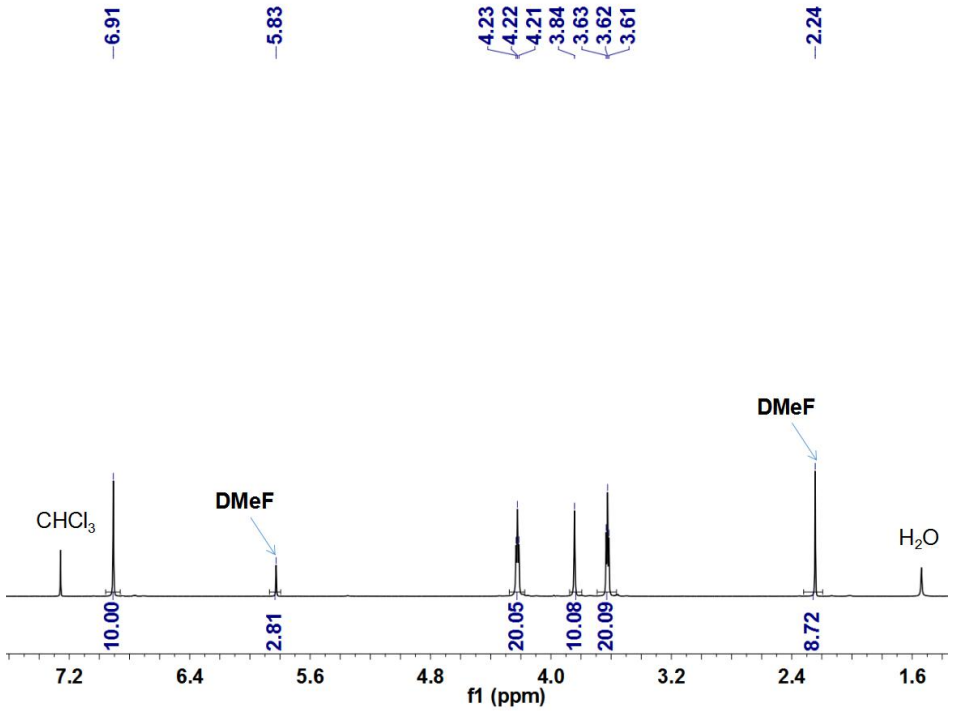


**Figure S18.** [1]H NMR spectrum (600 MHz, chloroform-*d*, 298 K) of **BrP5***α* after adsorption of **DMeF** vapor.

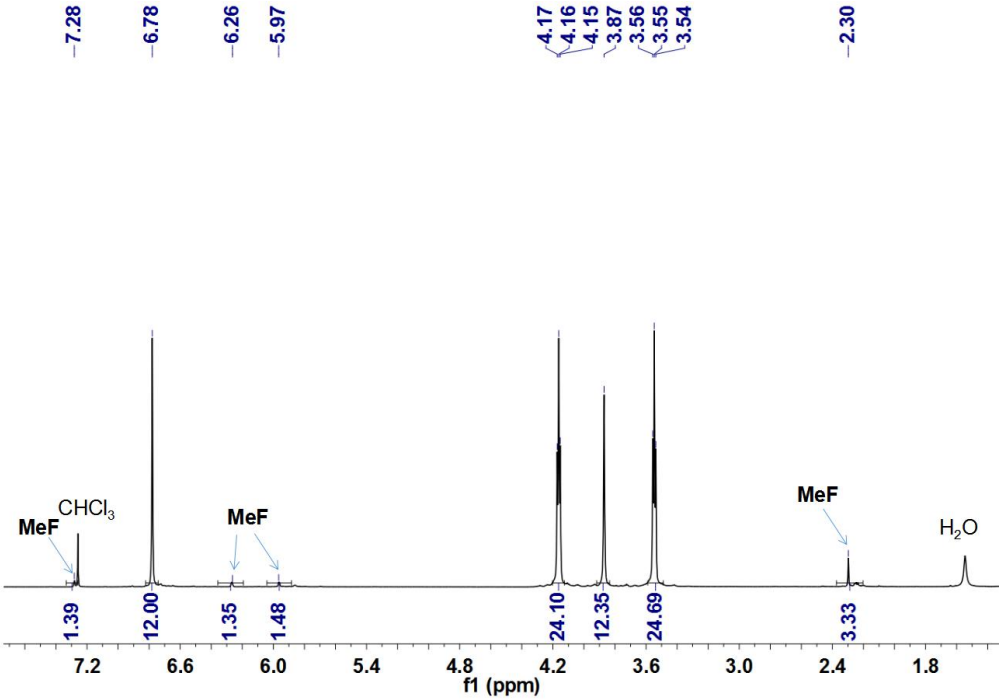


**Figure S19.** [1]H NMR spectrum (600 MHz, chloroform-*d*, 298 K) of **BrP6*β*** after adsorption of **MeF** vapor.

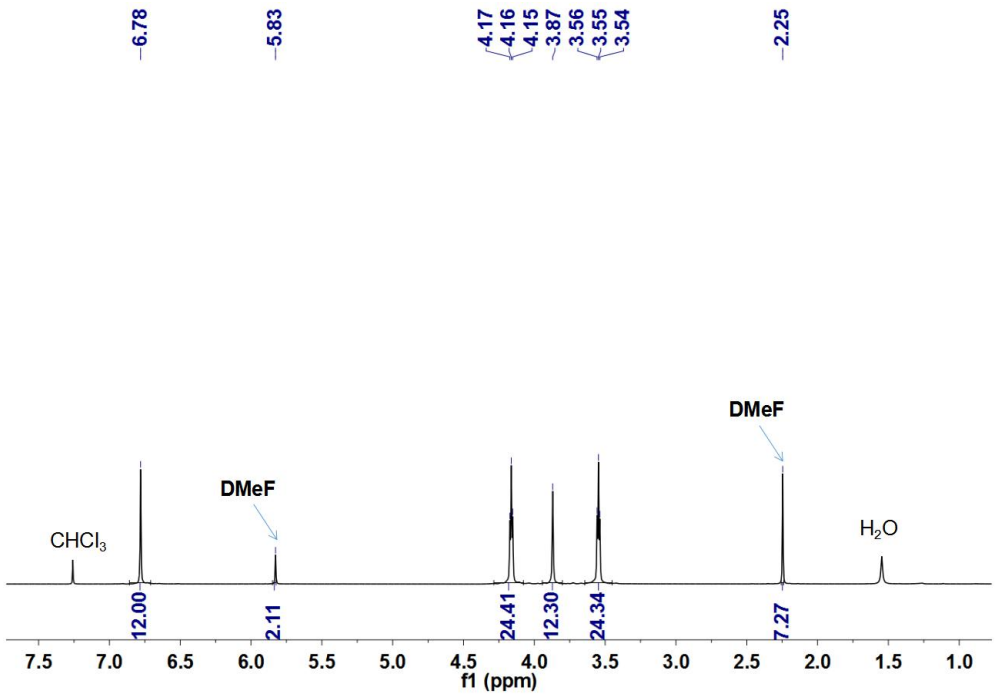


**Figure S20.** [1]H NMR spectrum (600 MHz, chloroform-*d*, 298 K) of **BrP6*β*** after adsorption of **DMeF** vapor.

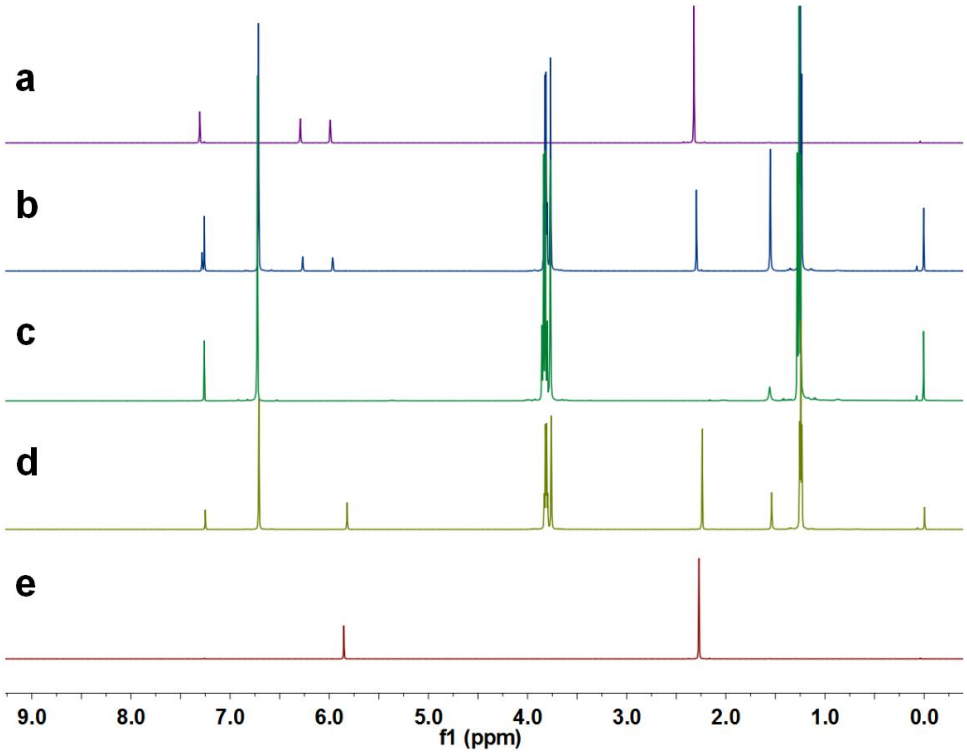


**Figure S21.** [1]H NMR spectra (400 MHz, chloroform-*d*, 298 K): (a) **MeF**; (b) **MeF** after mixing with **EtP5**; (c) **EtP5**; (d) **DMeF** after mixing with **EtP5**; (e) **DMeF**.

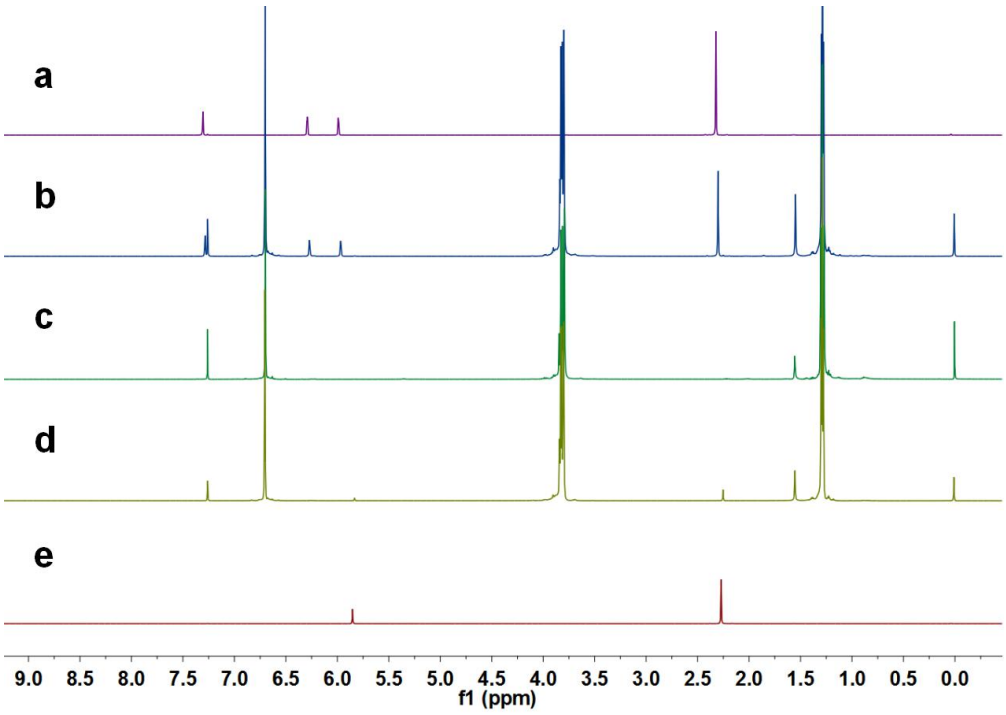


**Figure S22.** [1]H NMR spectra (400 MHz, chloroform-*d*, 298 K): (a) **MeF**; (b) **MeF** after mixing with **EtP6**; (c) **EtP6**; (d) **DMeF** after mixing with **EtP6**; (e) **DMeF**.

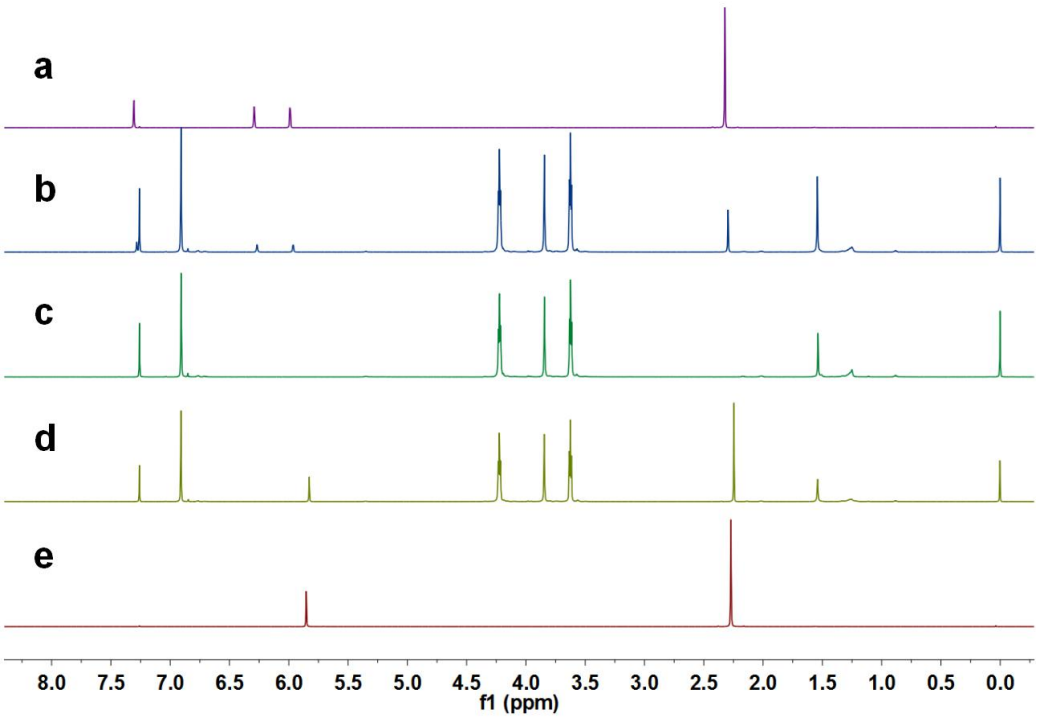


**Figure S23.** $^{1}$H NMR spectra (400 MHz, chloroform-*d*, 298 K): (a) **MeF**; (b) **MeF** after mixing with **BrP5**; (c) **BrP5**; (d) **DMeF** after mixing with **BrP5**; (e) **DMeF**.

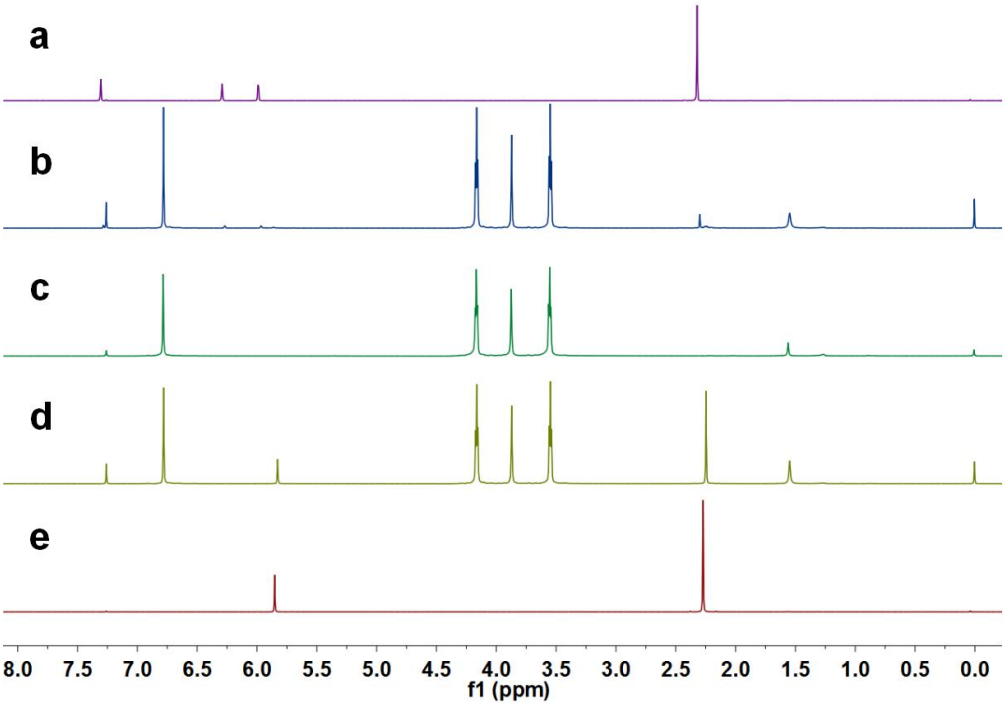


**Figure S24.** $^{1}$H NMR spectra (400 MHz, chloroform-*d*, 298 K): (a) **MeF**; (b) **MeF** after mixing with **BrP6**; (c) **BrP6**; (d) **DMeF** after mixing with **BrP6**; (e) **DMeF**.

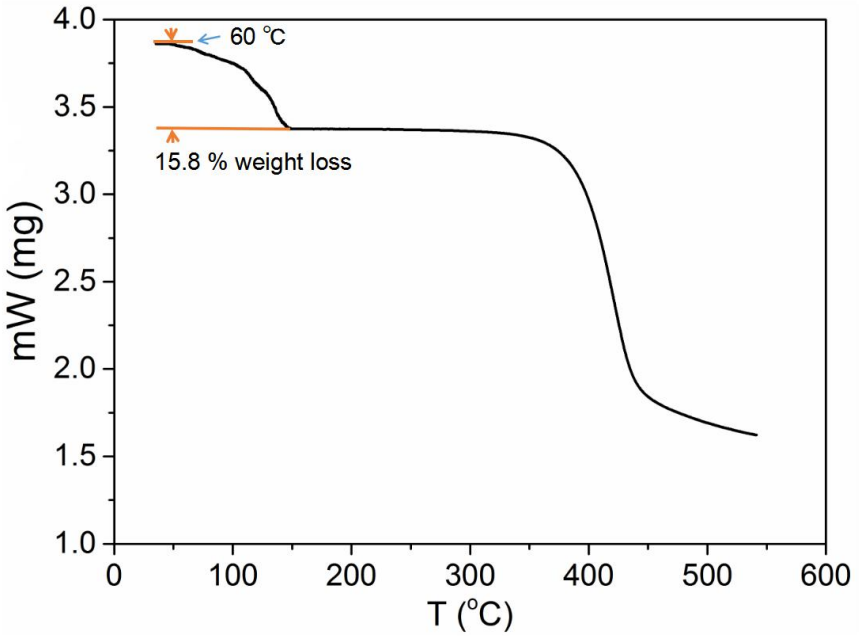


**Figure S25.** Thermogravimetric analysis of desolvated **EtP5***α* after sorption of **MeF** vapor. The weight loss below 150 °C can be calculated as two **MeF** molecules per **EtP5** molecule.

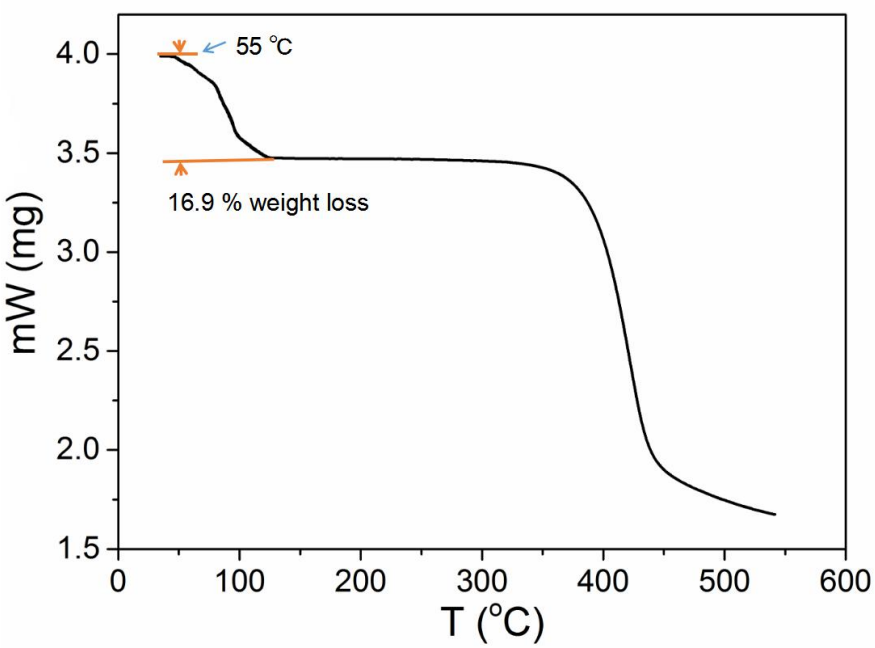


**Figure S26.** Thermogravimetric analysis of desolvated **EtP5***α* after sorption of **DMeF** vapor. The weight loss below 150 °C can be calculated as two **DMeF** molecules per **EtP5** molecule.

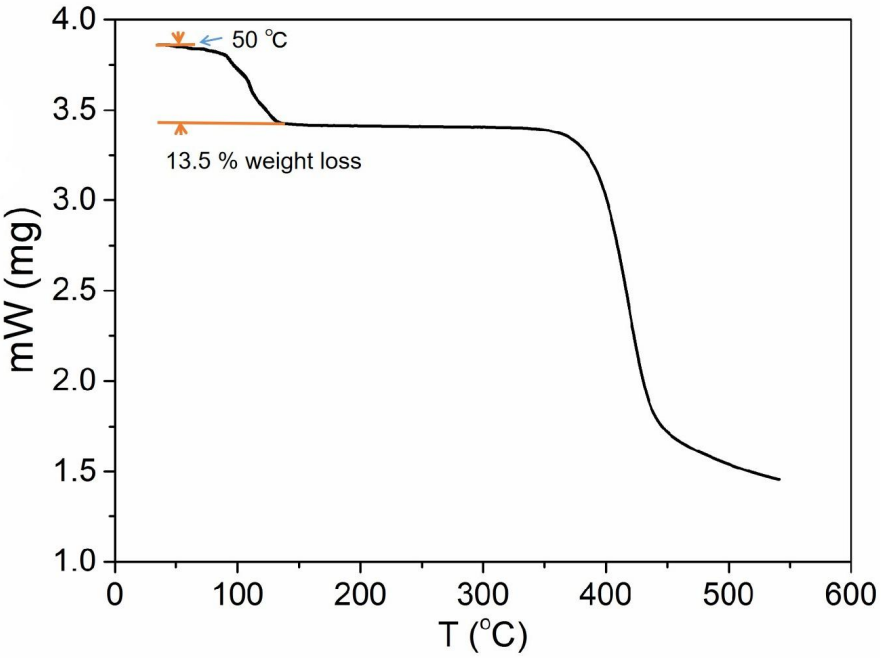


**Figure S27.** Thermogravimetric analysis of desolvated **EtP6***β* after sorption of **MeF** vapor. The weight loss below 150 °C can be calculated as two **MeF** molecules per **EtP6** molecule.

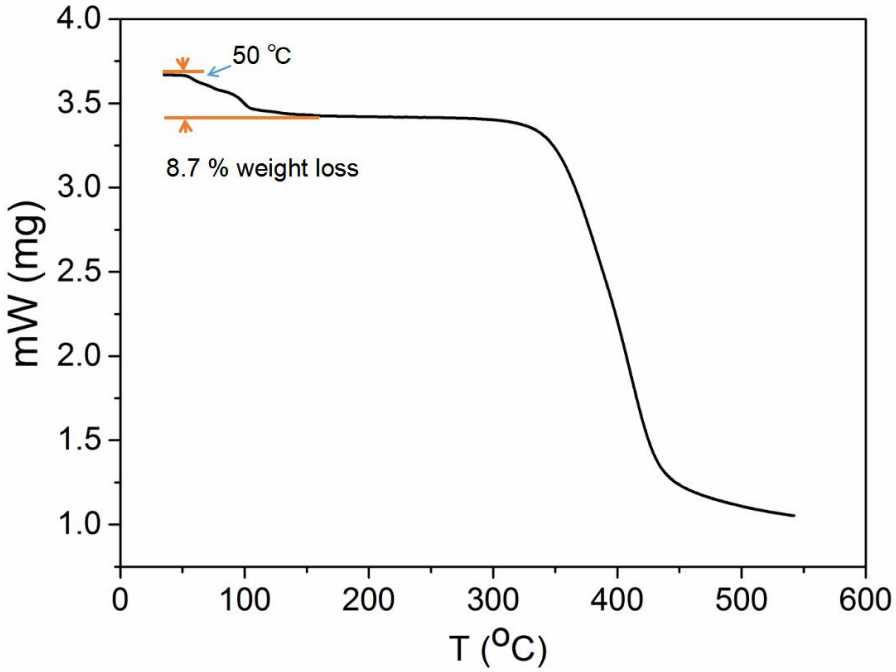


**Figure S28.** Thermogravimetric analysis of desolvated **EtP6***β* after sorption of **DMeF** vapor. The weight loss below 150 °C can be calculated as one **DMeF** molecule per **EtP6** molecule.

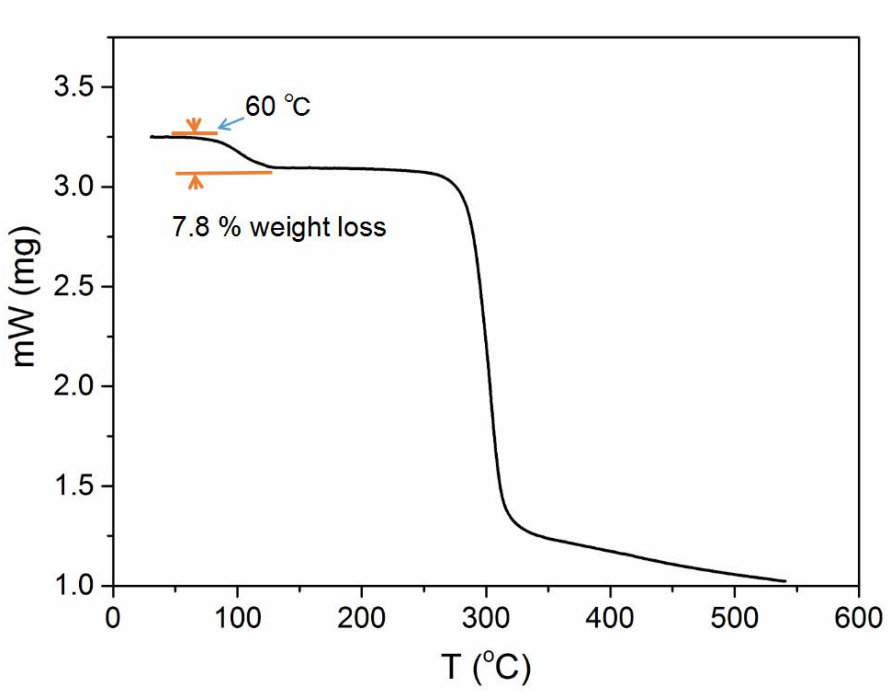


**Figure S29.** Thermogravimetric analysis of desolvated **BrP5***α* after sorption of **MeF** vapor. The weight loss below 150 °C can be calculated as two **MeF** molecules per **BrP5** molecule.

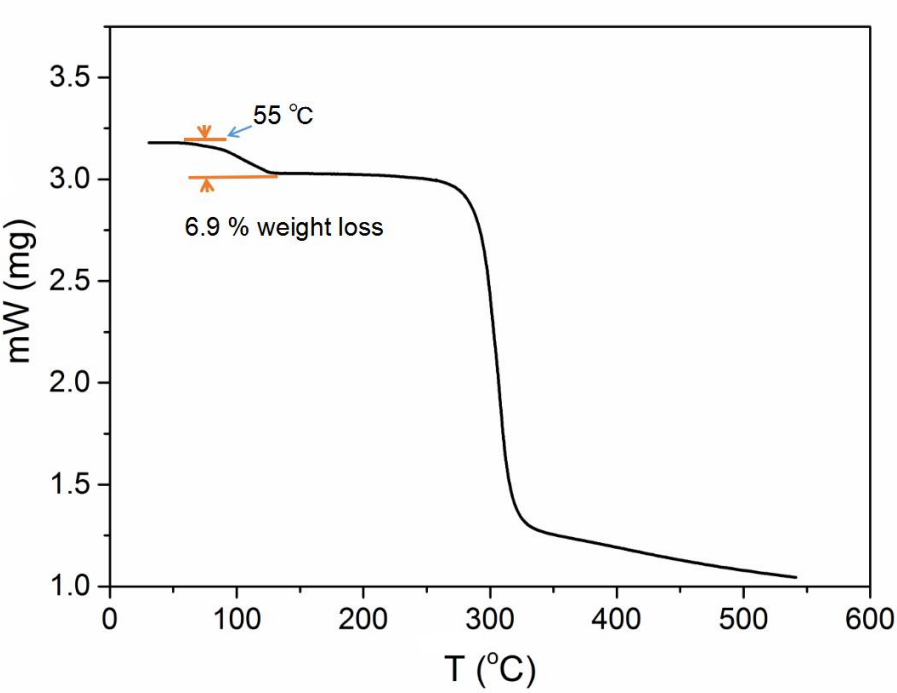


**Figure S30.** Thermogravimetric analysis of desolvated **BrP5***α* after sorption of **DMeF** vapor. The weight loss below 150 °C can be calculated as two **DMeF** molecules per **BrP5** molecule.

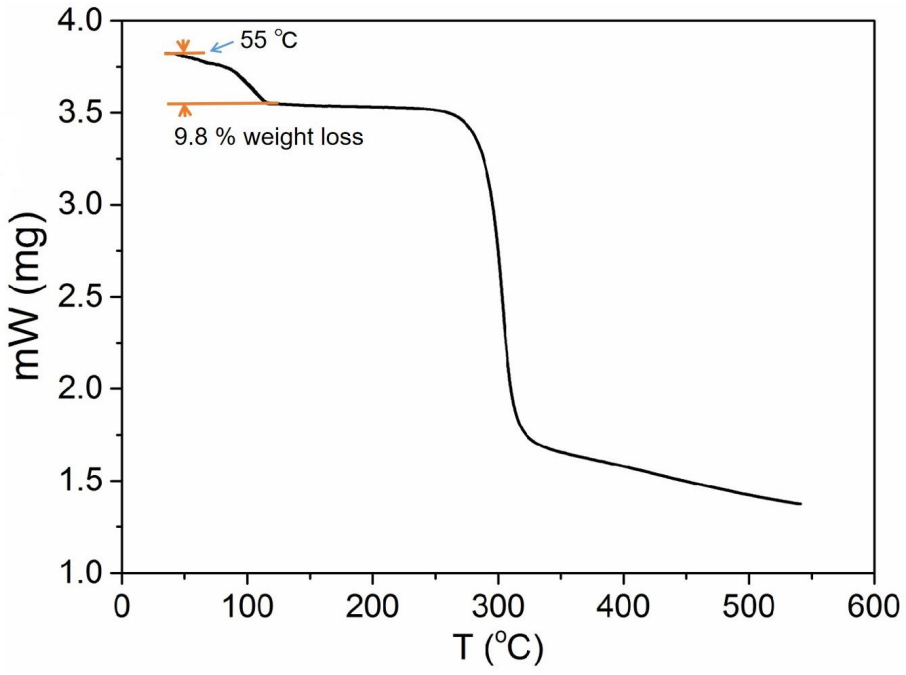


**Figure S31.** Thermogravimetric analysis of desolvated **BrP6***β* after sorption of **MeF** vapor. The weight loss below 150 °C can be calculated as two **MeF** molecules per **BrP6** molecule.

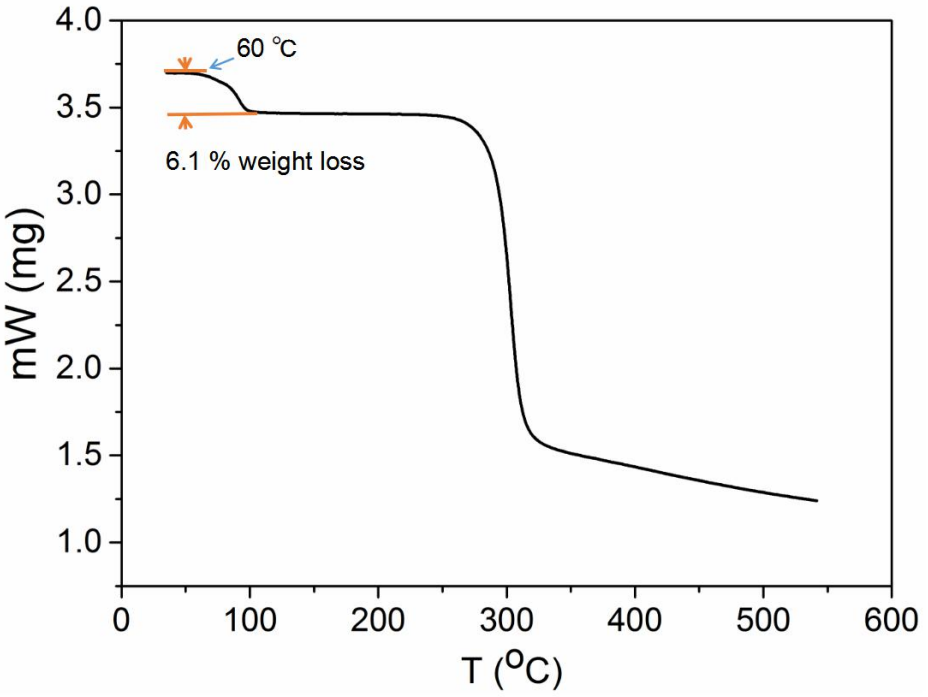


**Figure S32.** Thermogravimetric analysis of desolvated **BrP6***β* after sorption of **DMeF** vapor. The weight loss below 150 °C can be calculated as one **DMeF** molecule per **BrP6** molecule.

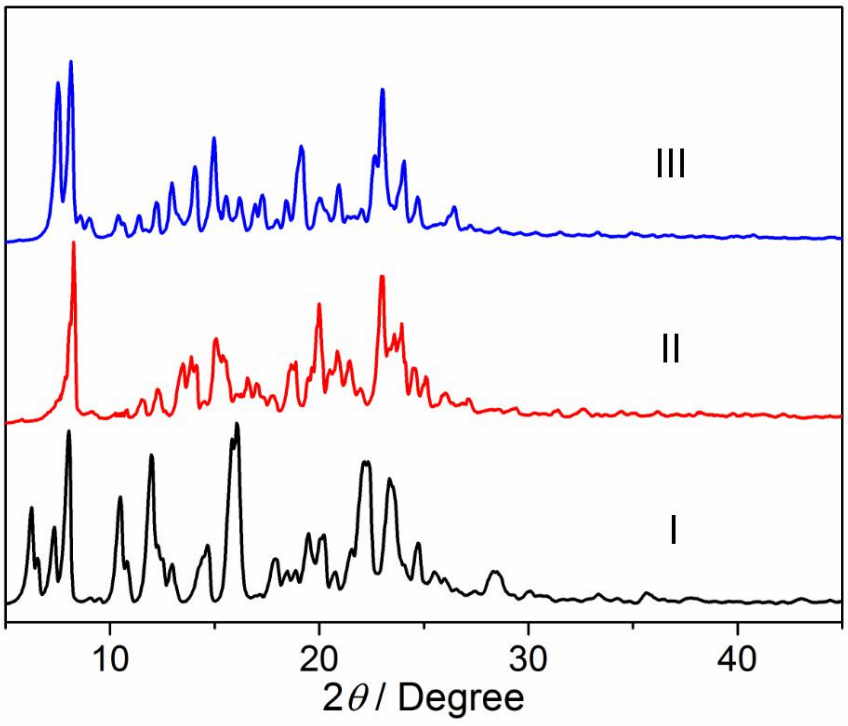


**Figure S33.** Powder X-ray diffraction patterns of **EtP5**: (I) original **EtP5***α*; (II) after adsorption of **MeF** vapor; (III) after adsorption of **DMeF** vapor.

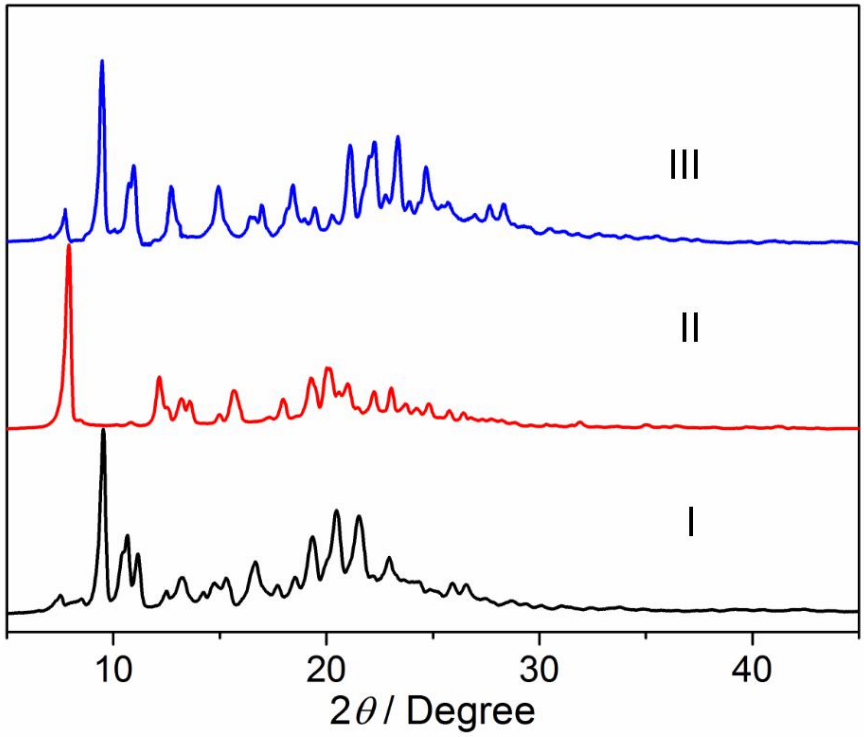


**Figure S34.** Powder X-ray diffraction patterns of **EtP6**: (I) original **EtP6***β*; (II) after adsorption of **MeF** vapor; (III) after adsorption of **DMeF** vapor.

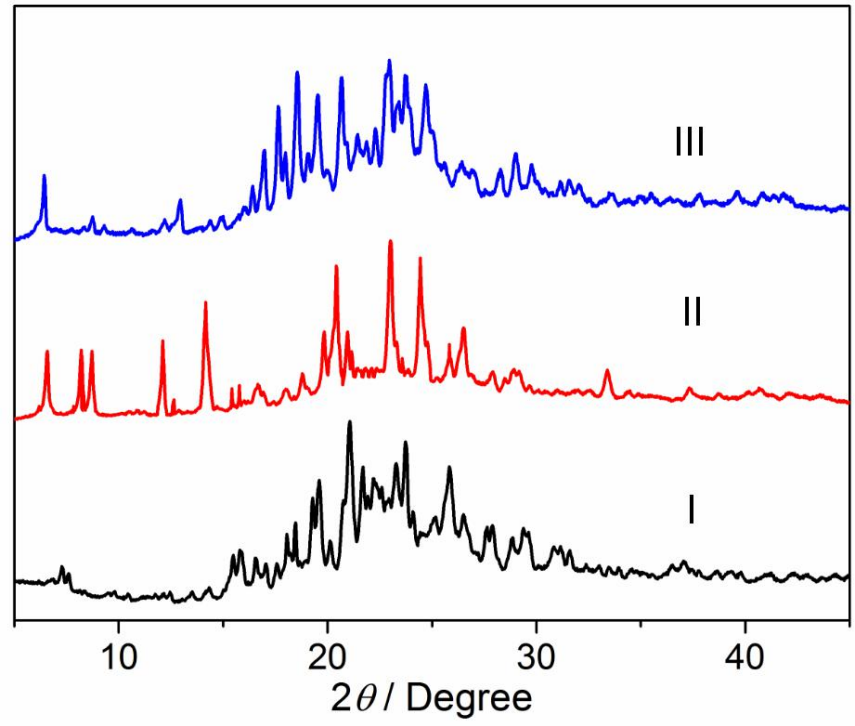


**Figure S35.** Powder X-ray diffraction patterns of **BrP5**: (I) original **BrP5***α*; (II) after adsorption of **MeF** vapor; (III) after adsorption of **DMeF** vapor.

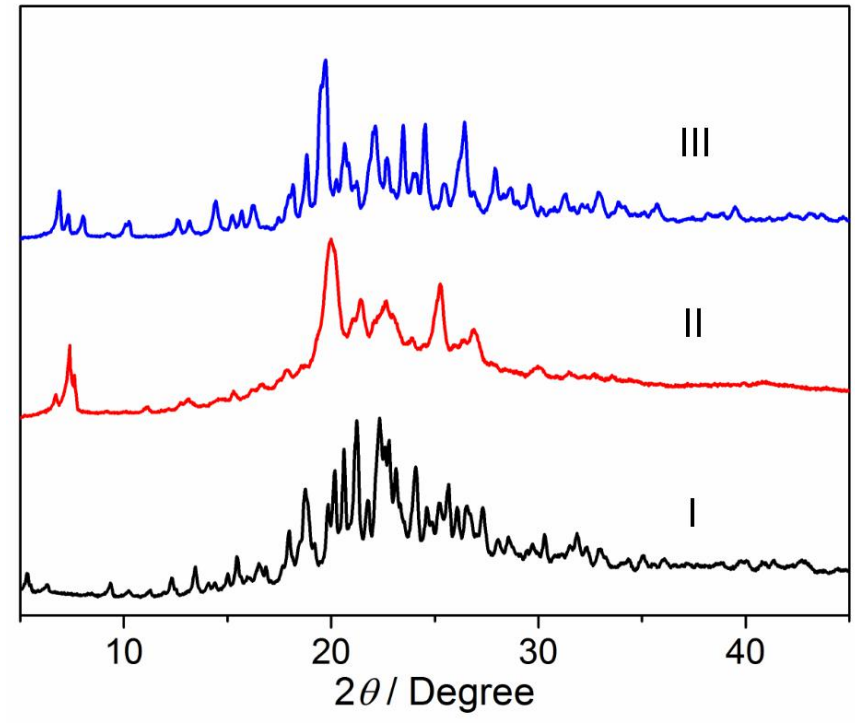


**Figure S36.** Powder X-ray diffraction patterns of **BrP6**: (I) original **BrP6***β*; (II) after adsorption of **MeF** vapor (disorder); (III) after adsorption of **DMeF** vapor.

*5.2. Structural Analyses after Single-Component Vapor Sorption*

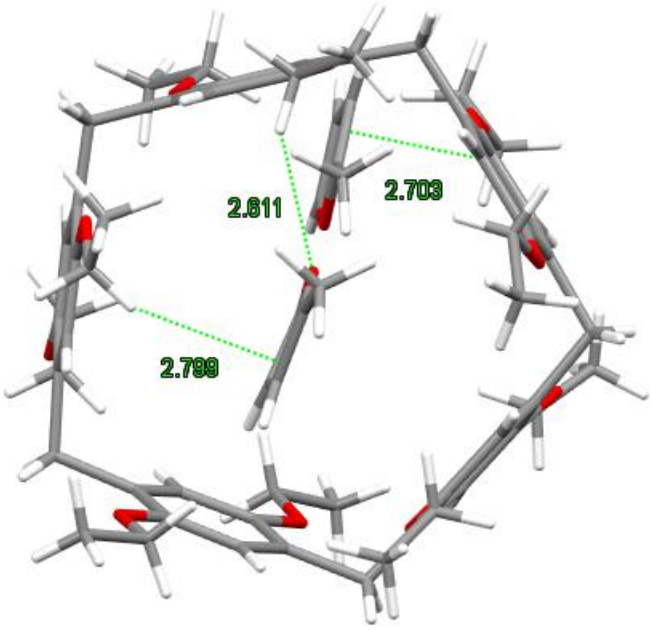


**Figure S37.** Single crystal structure of **(MeF)$_2$@EtP5**. H···O distance (Å) and C–H···O angle (deg) of hydrogen bond: 2.611, 145.48; C–H···π distances (Å): 2.703, 2.799.

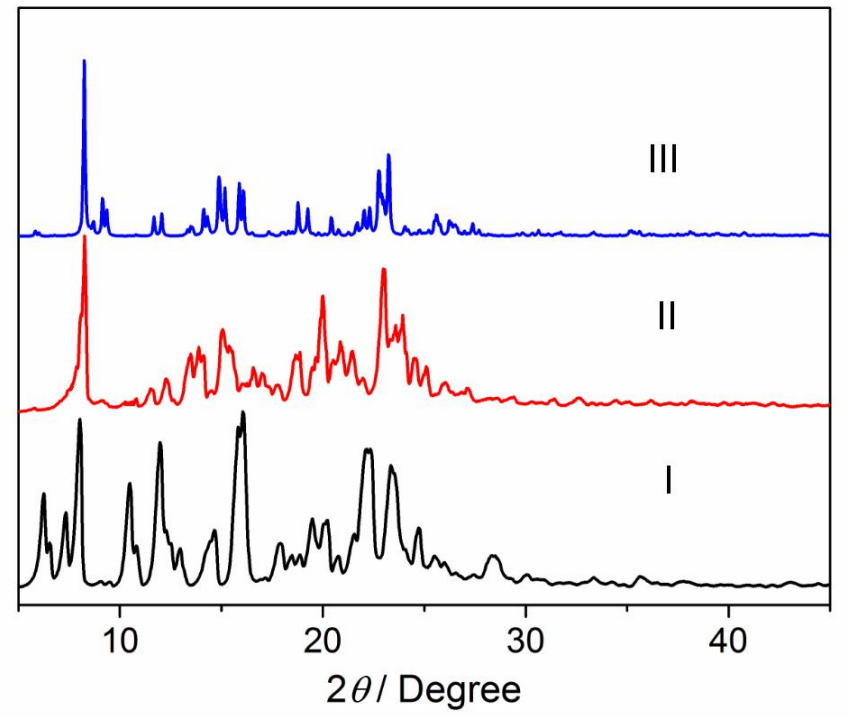


**Figure S38.** Powder X-ray diffraction patterns of **EtP5**: (I) original **EtP5**$\alpha$; (II) after adsorption of **MeF** vapor; (III) simulated from single crystal structure of **(MeF)$_2$@EtP5**.

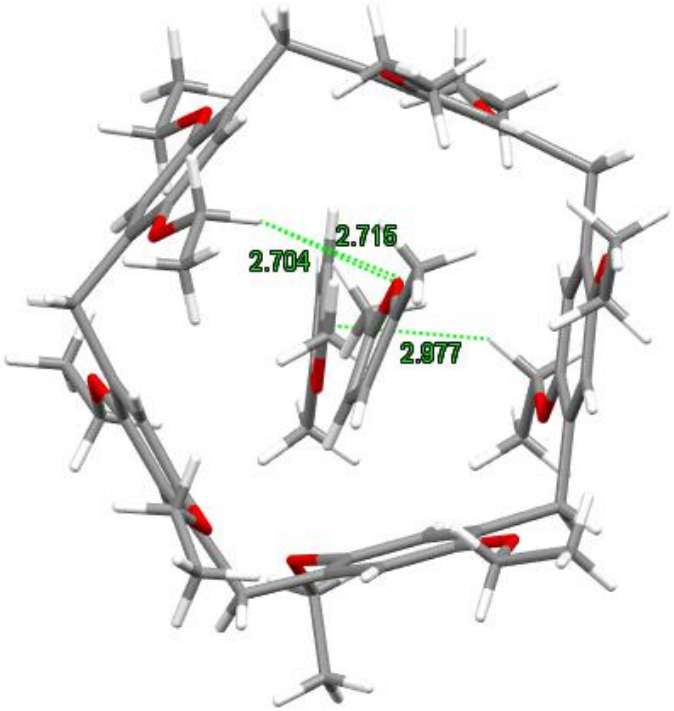


**Figure S39.** Single crystal structure of **(DMeF)$_2$@EtP5**. H···O distance (Å) and C–H···O angle (deg) of hydrogen bond: 2.715, 159.70; C–H···π distances (Å): 2.704, 2.982.

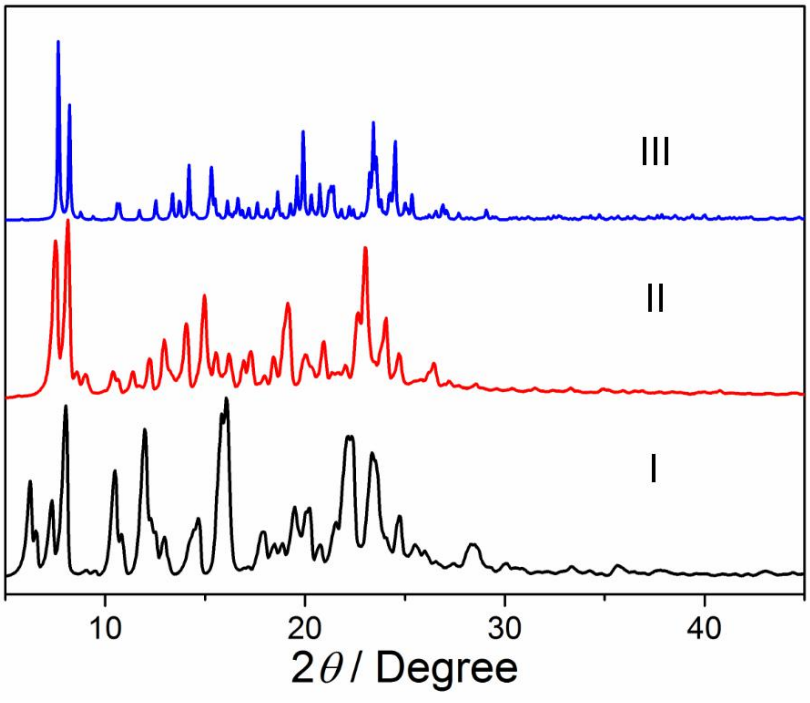


**Figure S40.** Powder X-ray diffraction patterns of **EtP5**: (I) original **EtP5***α*; (II) after adsorption of **DMeF** vapor; (III) simulated from single crystal structure of **(DMeF)$_2$@EtP5**.

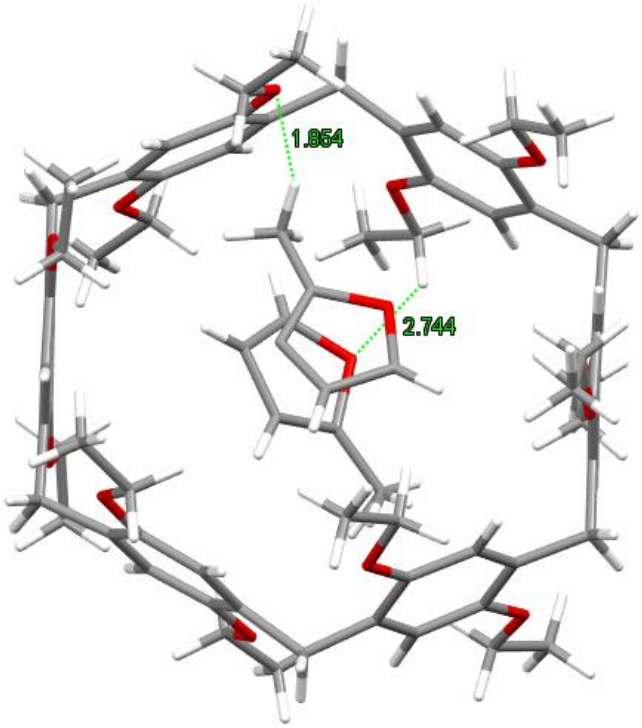


**Figure S41.** Single crystal structure of **(MeF)$_2$@EtP6**. H···O distances (Å) and C–H···O angles (deg) of hydrogen bonds: 1.854, 150.46; 2.744, 134.85.

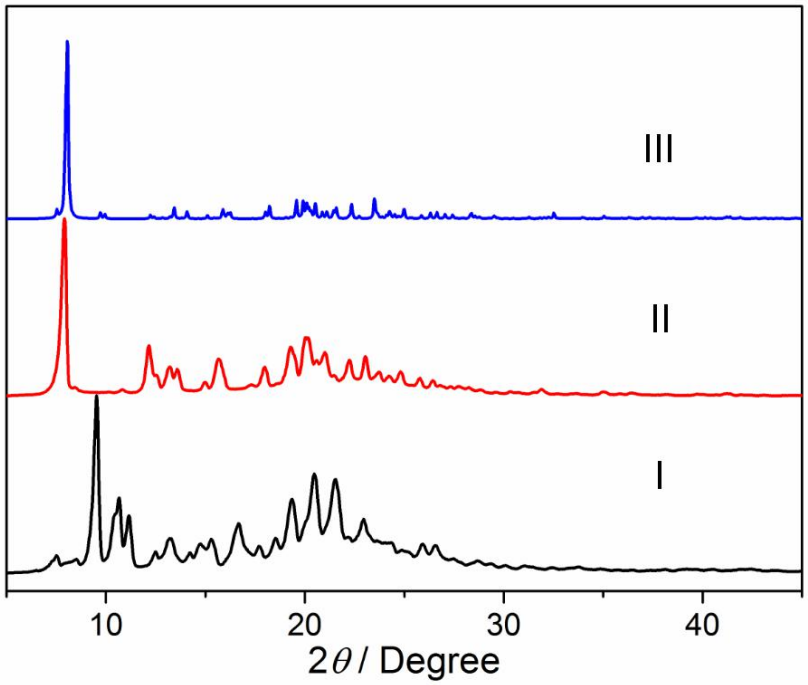


**Figure S42.** Powder X-ray diffraction patterns of **EtP6**: (I) original **EtP6**$\beta$; (II) after adsorption of **MeF** vapor; (III) simulated from single crystal structure of **(MeF)$_2$@EtP6**.

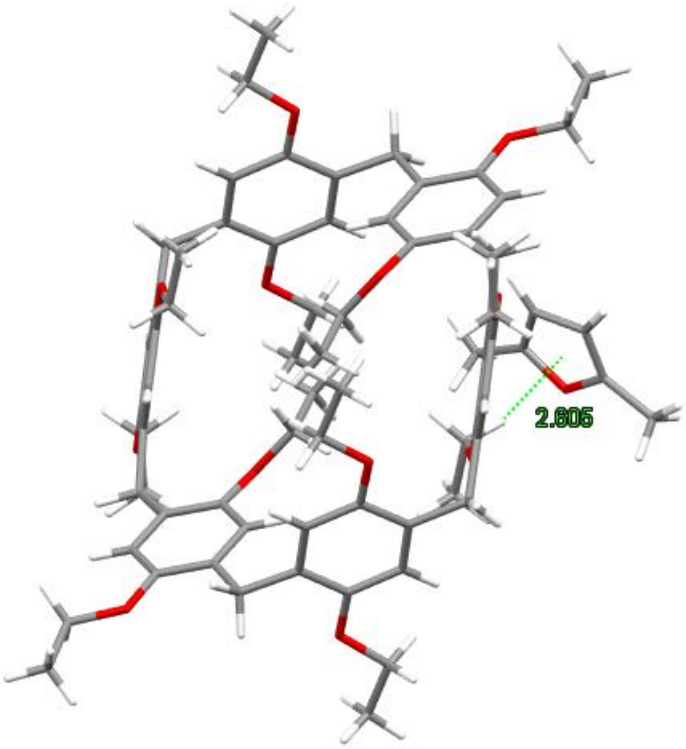


**Figure S43.** Single crystal structure of **DMeF@EtP6**. C–H···π distance (Å): 2.605.

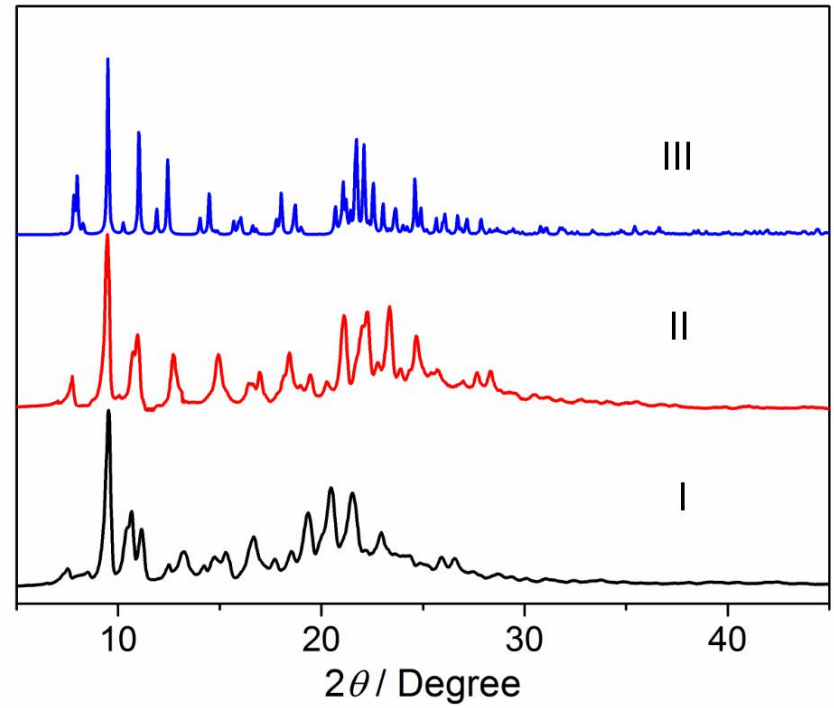


**Figure S44.** Powder X-ray diffraction patterns of **EtP6**: (I) original **EtP6***β*; (II) after adsorption of **DMeF** vapor; (III) simulated from single crystal structure of **DMeF@EtP6**.

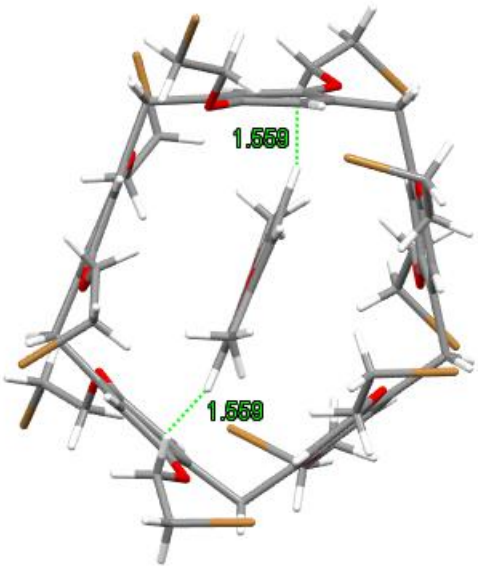


**Figure S45.** Single crystal structure of **(MeF)$_2$@BrP5**. C–H···π distances (Å): 1.559, 1.559.

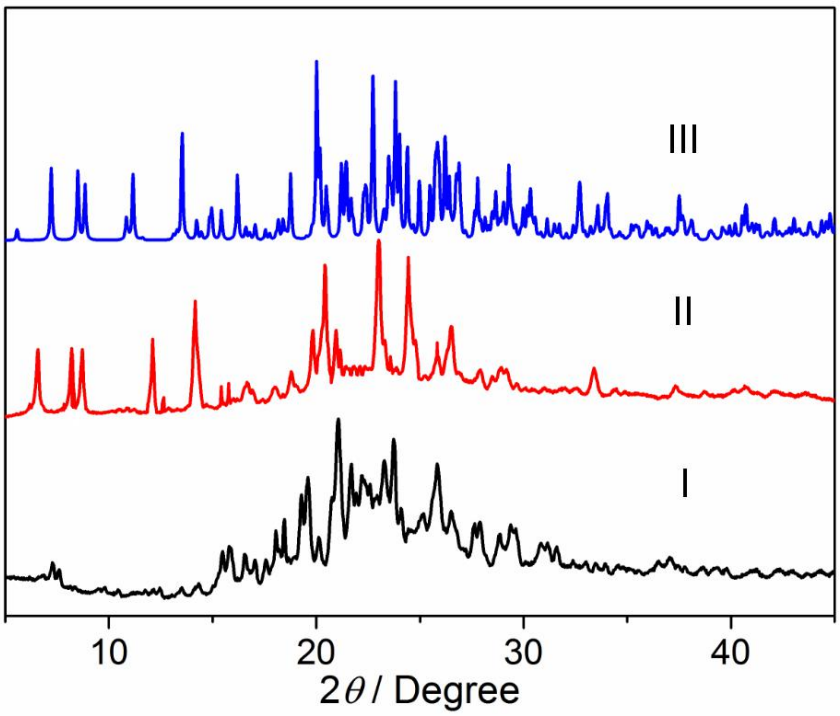


**Figure S46.** Powder X-ray diffraction patterns of **BrP5**: (I) original **BrP5**$\alpha$; (II) after adsorption of **MeF** vapor; (III) simulated from single crystal structure of **(MeF)$_2$@BrP5**.

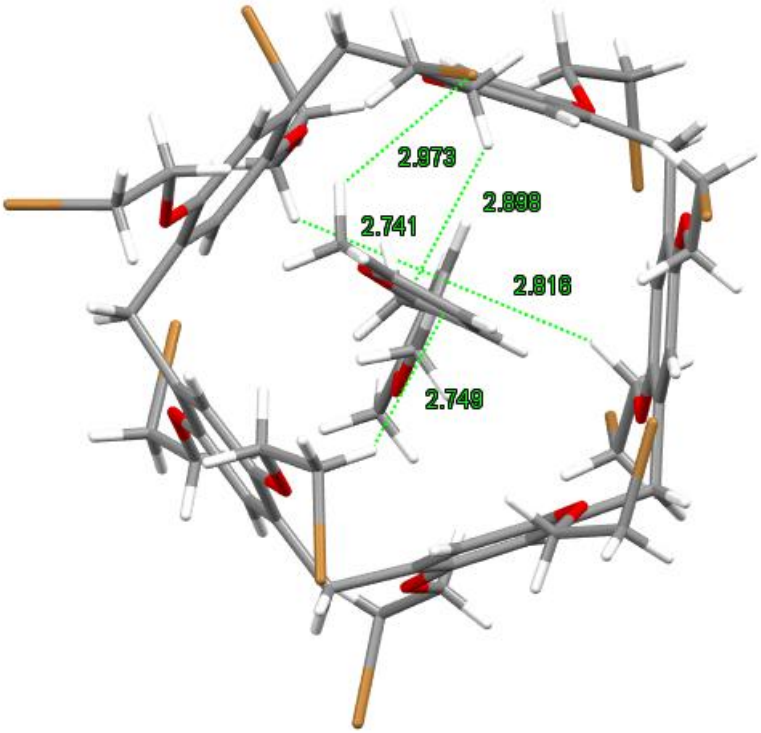


**Figure S47.** Single crystal structure of **(DMeF)$_2$@BrP5**. H···Br distance (Å) and C–H···Br angle (deg) of hydrogen bond: 2.973, 128.65; C–H···π distances (Å): 2.741, 2.749, 2.816, 2.898.

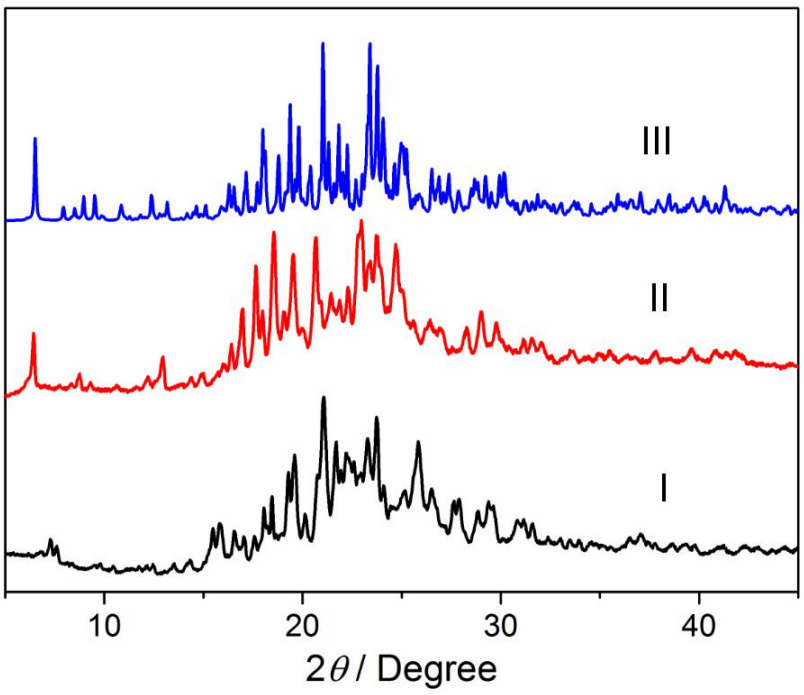


**Figure S48.** Powder X-ray diffraction patterns of **BrP5**: (I) original **BrP5**$\alpha$; (II) after adsorption of **DMeF** vapor; (III) simulated from single crystal structure of **(DMeF)$_2$@BrP5**.

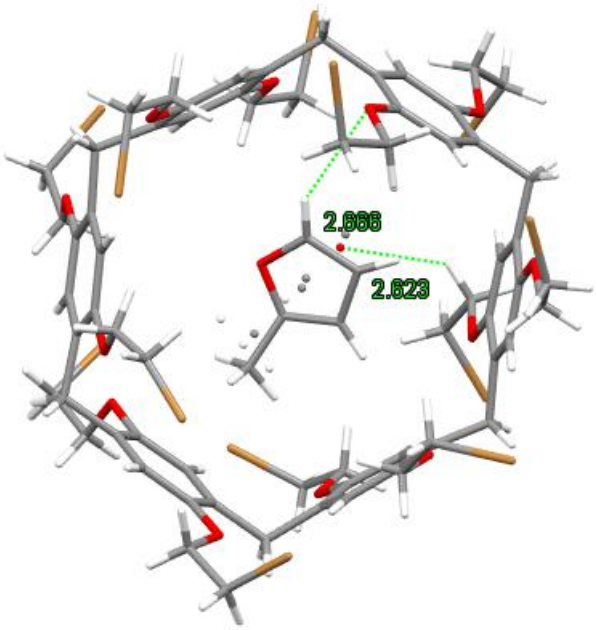


**Figure S49.** Single crystal structure of **(MeF)$_2$@BrP6** (disorder). H···O distances (Å) and C–H···O angles (deg) of hydrogen bonds: 2.623, 132.93; 2.666, 142.14.

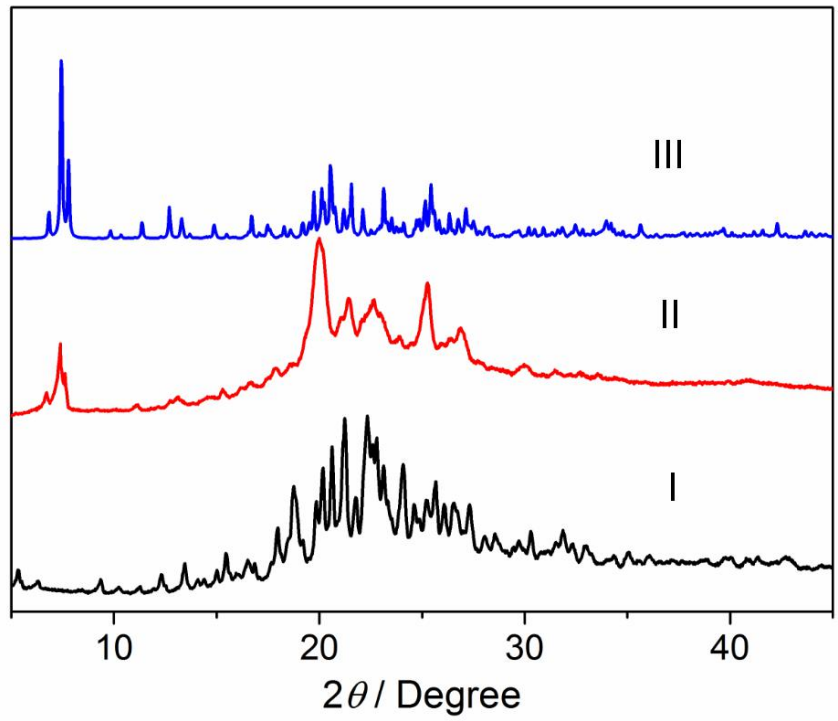


**Figure S50.** Powder X-ray diffraction patterns of **BrP6**: (I) original **BrP6**$\beta$; (II) after adsorption of **MeF** vapor; (III) simulated from single crystal structure of **(MeF)$_2$@BrP6**.

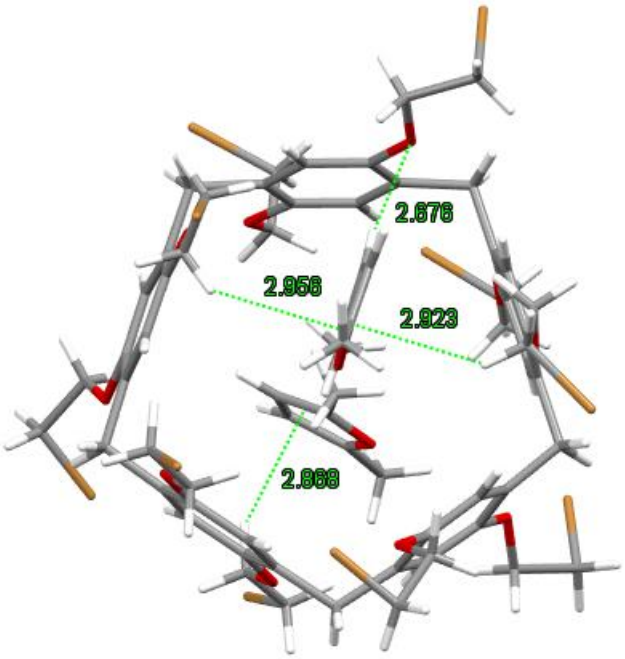


**Figure S51.** Single crystal structure of **(DMeF)$_2$@BrP6**. H···O distance (Å) and C–H···O angle (deg) of hydrogen bond: 2.676, 172.77; C–H···π distances (Å) : 2.868, 2.923, 2.956.

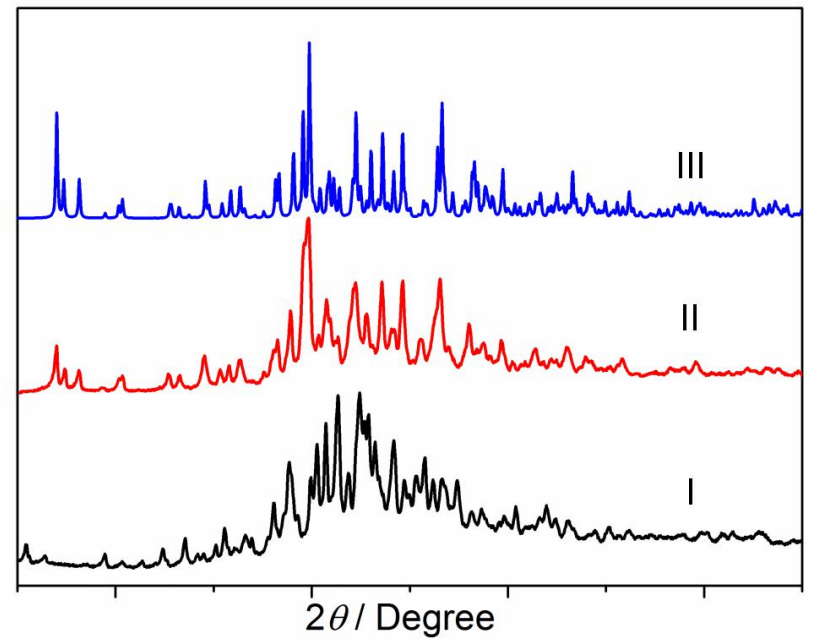


**Figure S52.** Powder X-ray diffraction patterns of **BrP6**: (I) original **BrP6***β*; (II) after adsorption of **DMeF** vapor; (III) simulated from single crystal structure of **DMeF@BrP6**.

*5.3. Uptake from **MeF** and **DMeF** in **EtP5**α*

For each vapor-phase mixture experiment, an open 5.00 mL vial containing 20.00 mg of guest-free **EtP5**α adsorbent was placed in a sealed 20.00 mL vial containing 1.00 mL of a 50:50 *v/v* **MeF** and **DMeF** mixture. The relative uptake of **MeF** or **DMeF** by **EtP5**α was measured by heating the crystals to release the adsorbed vapor using gas chromatography. Before measurements, the crystals were heated at 60 ℃ to remove the surface-physically adsorbed vapor.

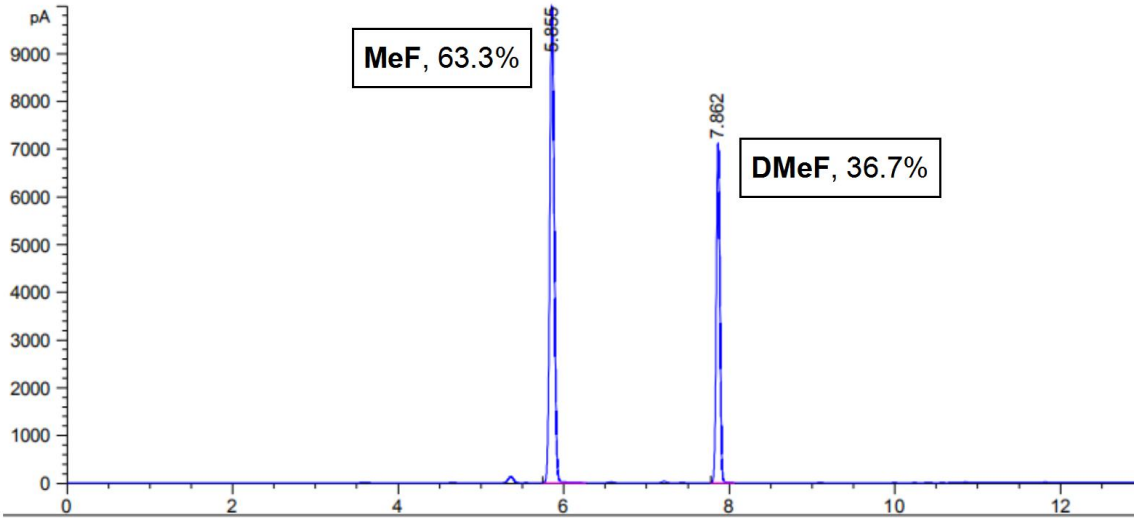


**Figure S53.** Relative uptake of the **MeF**/**DMeF** mixture (*v*:*v* = 50:50) adsorbed in **EtP5**α after 24 hours using gas chromatography.

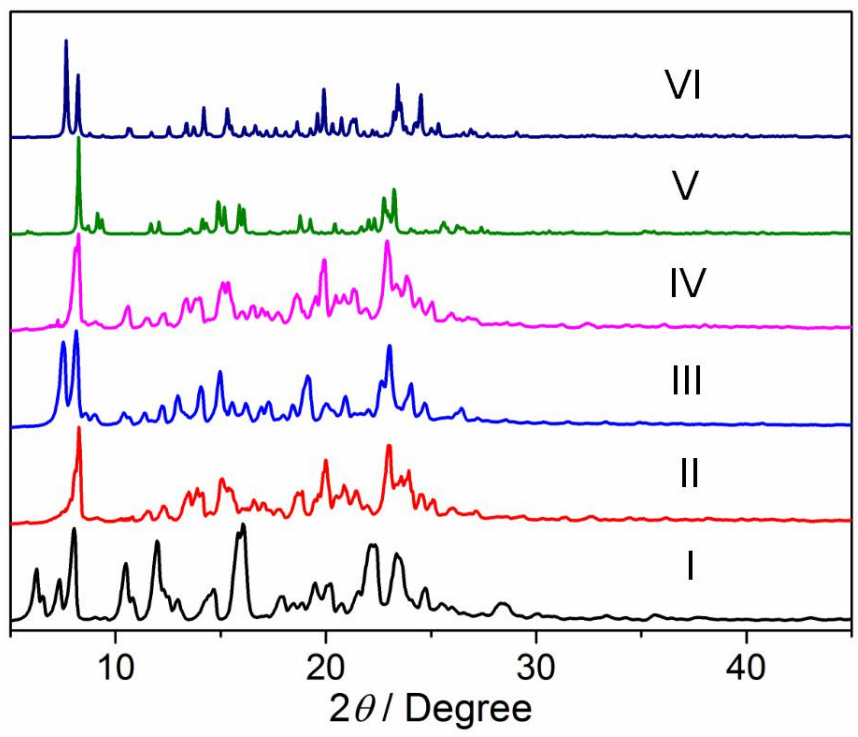


**Figure S54.** Powder X-ray diffraction patterns of **EtP5**: (I) original **EtP5***α*; (II) after adsorption of **MeF** vapor; (III) after adsorption of **DMeF** vapor; (IV) after adsorption of a 50:50 *v/v* **MeF** and **DMeF** mixture vapor; (V) simulated from single crystal structure of **(MeF)$_2$@EtP5**; (VI) simulated from single crystal structure of **(DMeF)$_2$@EtP5**.

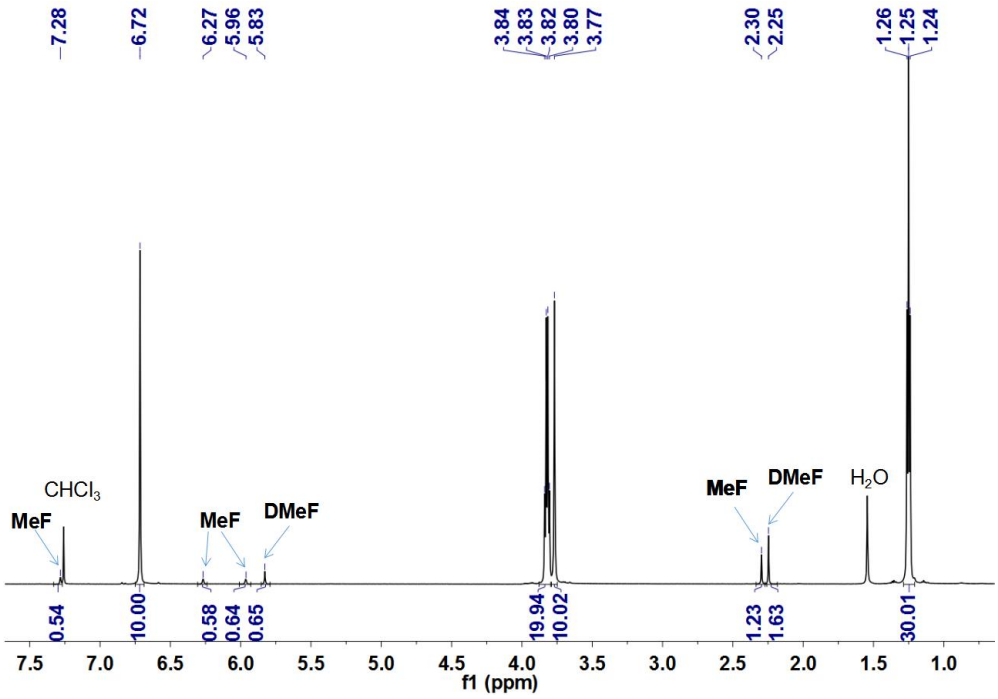


**Figure S55.** $^1$H NMR spectrum (600 MHz, chloroform-*d*, 298 K) of **EtP5***α* after adsorption of a 50:50 *v/v* **MeF** and **DMeF** mixture vapor.

*5.4. Uptake from **MeF** and **DMeF** in **EtP6β***

For each vapor-phase mixture experiment, an open 5.00 mL vial containing 20.00 mg of guest-free **EtP6*β*** adsorbent was placed in a sealed 20.00 mL vial containing 1.00 mL of a 50:50 *v/v* **MeF** and **DMeF** mixture. The relative uptake of **MeF** or **DMeF** by **EtP6*β*** was measured by heating the crystals to release the adsorbed vapor using gas chromatography. Before measurements, the crystals were heated at 60 ℃ to remove the surface-physically adsorbed vapor.

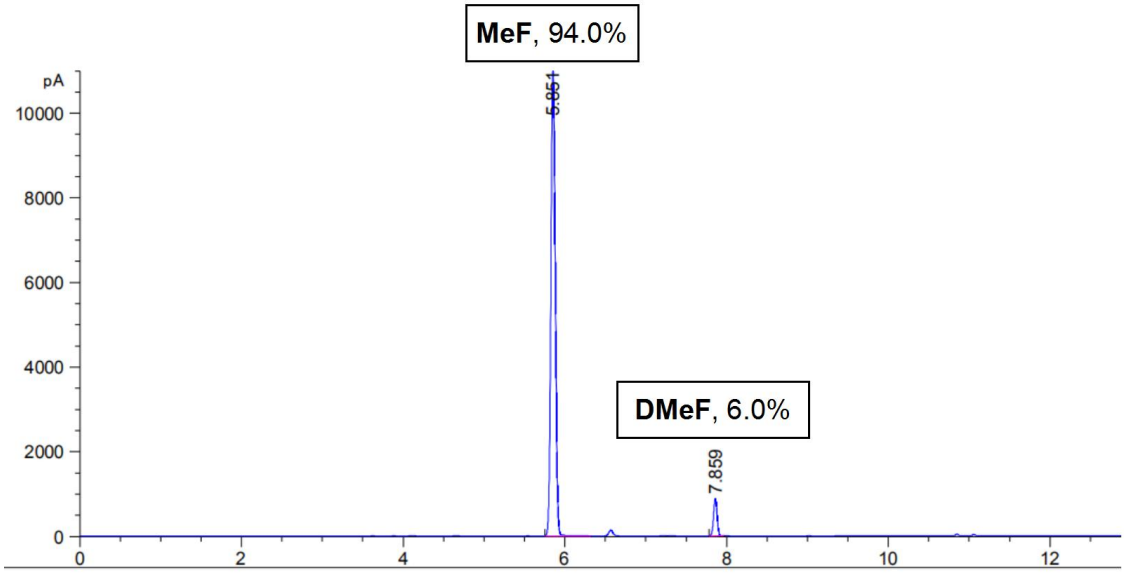


**Figure S56.** Relative uptake of the **MeF**/**DMeF** mixture (*v*:*v* = 50:50) adsorbed in **EtP6*β*** after 24 hours using gas chromatography.

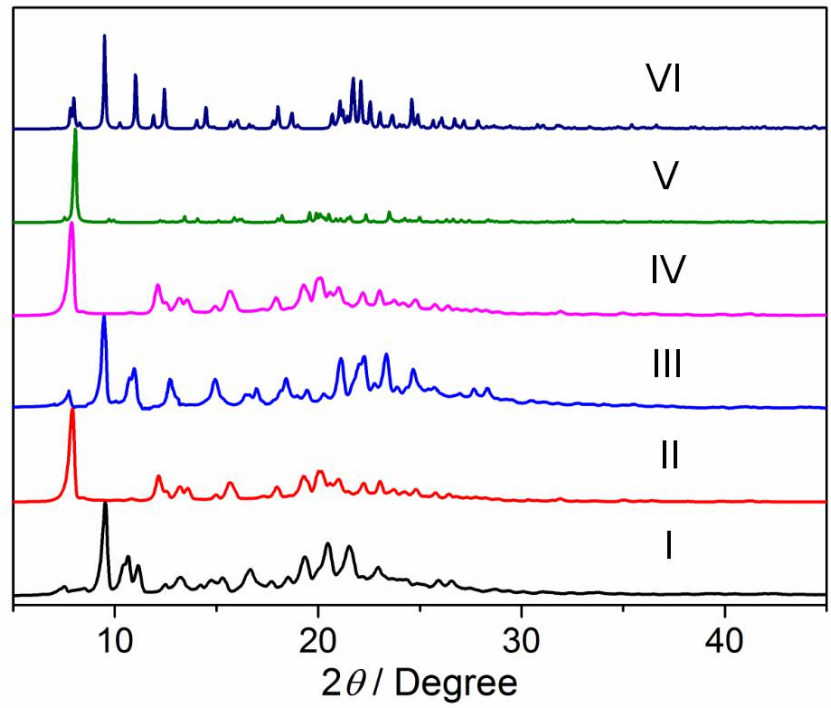

**Figure S57.** Powder X-ray diffraction patterns of **EtP6**: (I) original **EtP6***β*; (II) after adsorption of **MeF** vapor; (III) after adsorption of **DMeF** vapor; (IV) after adsorption of a 50:50 *v/v* **MeF** and **DMeF** mixture vapor; (V) simulated from single crystal structure of **(MeF)$_2$@EtP6**; (VI) simulated from single crystal structure of **DMeF@EtP6**.

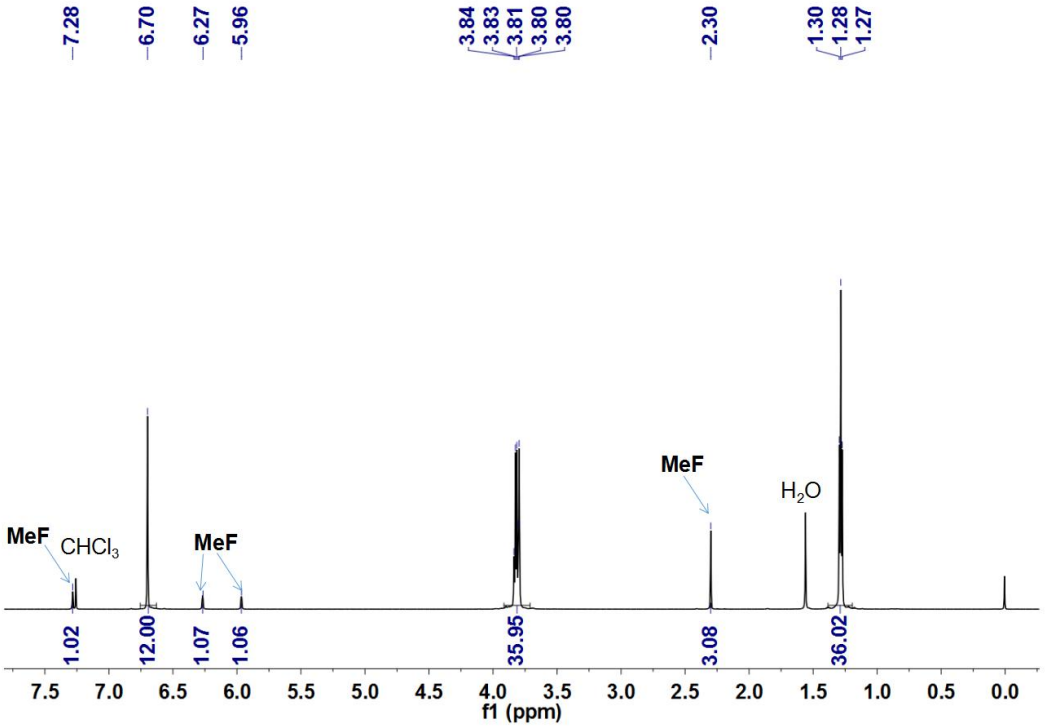


**Figure S58.** $^1$H NMR spectrum (600 MHz, chloroform-*d*, 298 K) of **EtP6***β* after adsorption of a 50:50 *v/v* **MeF** and **DMeF** mixture vapor.

*5.5. Uptake from **MeF** and **DMeF** in **BrP5**α*

For each vapor-phase mixture experiment, an open 5.00 mL vial containing 20.00 mg of guest-free **BrP5***α* adsorbent was placed in a sealed 20.00 mL vial containing 1.00 mL of a 50:50 *v/v* **MeF** and **DMeF** mixture. The relative uptake of **MeF** or **DMeF** by **BrP5***α* was measured by heating the crystals to release the adsorbed vapor using gas chromatography. Before measurements, the crystals were heated at 60 ℃ to remove the surface-physically adsorbed vapor.

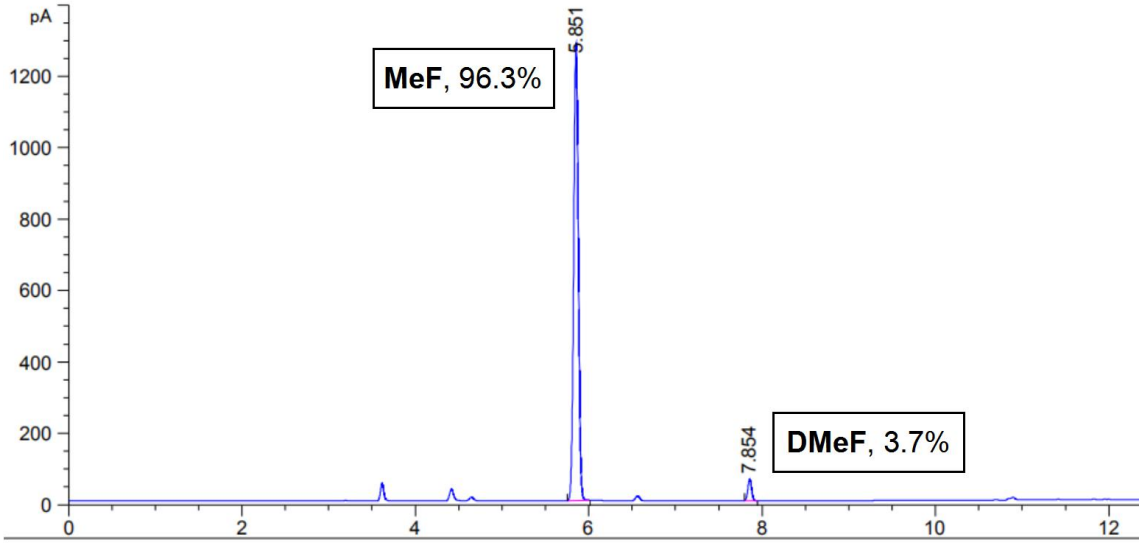


**Figure S59.** Relative uptake of the **MeF**/**DMeF** mixture (*v*:*v* = 50:50) adsorbed in **BrP5***α* after 24 hours using gas chromatography.

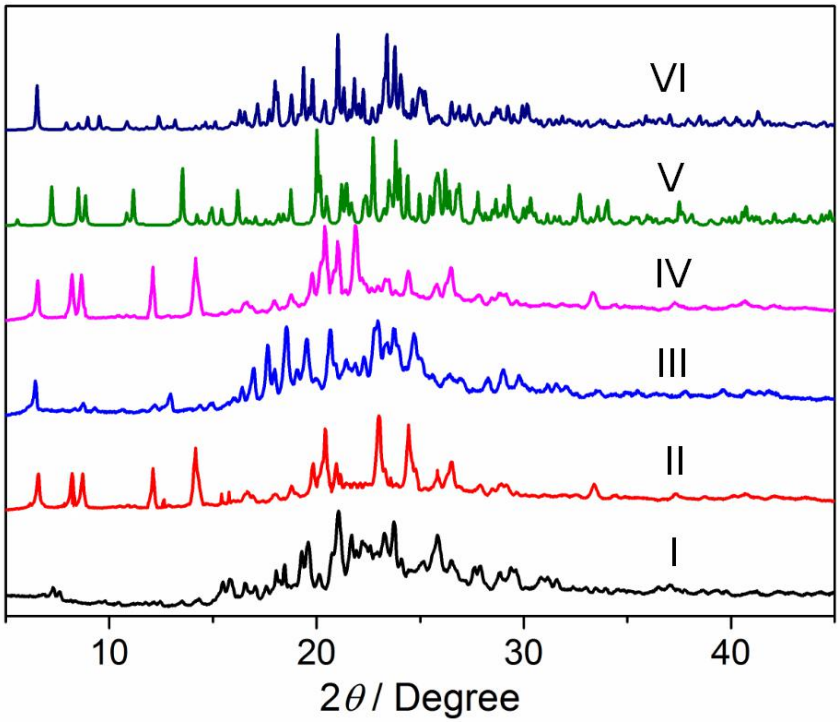


**Figure S60.** Powder X-ray diffraction patterns of **BrP5**: (I) original **BrP5***α*; (II) after adsorption of **MeF** vapor; (III) after adsorption of **DMeF** vapor; (IV) after adsorption of a 50:50 *v*/*v* **MeF** and **DMeF** mixture vapor; (V) simulated from single crystal structure of **(MeF)$_2$@BrP5**; (VI) simulated from single crystal structure of **(DMeF)$_2$@BrP5**.

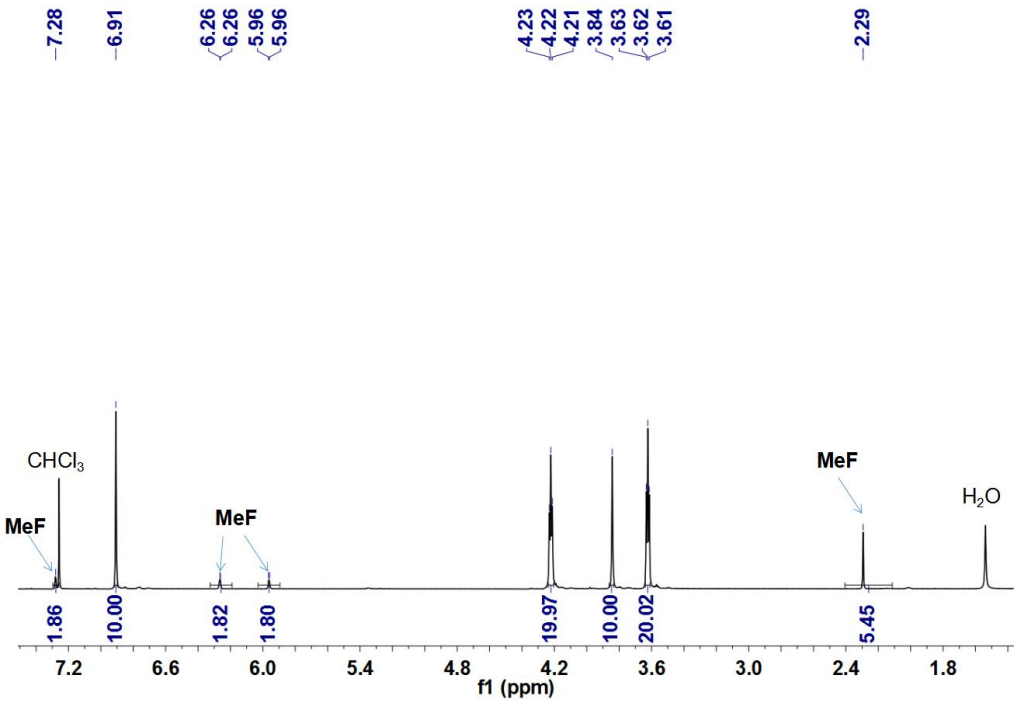


**Figure S61.** [1]H NMR spectrum (600 MHz, chloroform-*d*, 298 K) of **BrP5***α* after adsorption of a 50:50 *v/v* **MeF** and **DMeF** mixture vapor.

*5.6. Uptake from **MeF** and **DMeF** in **BrP6**β*

For each vapor-phase mixture experiment, an open 5.00 mL vial containing 20.00 mg of guest-free **BrP6***β* adsorbent was placed in a sealed 20.00 mL vial containing 1.00 mL of a 50:50 *v/v* **MeF** and **DMeF** mixture. The relative uptake of **MeF** or **DMeF** by **BrP6***β* was measured by heating the crystals to release the adsorbed vapor using gas chromatography. Before measurements, the crystals were heated at 60 ℃ to remove the surface-physically adsorbed vapor.

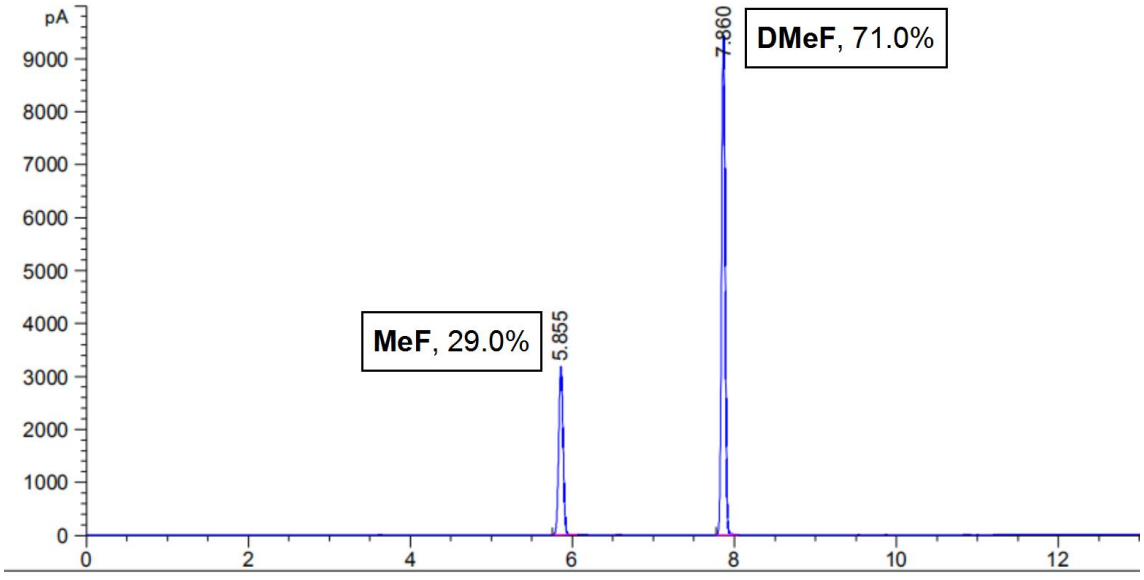

**Figure S62.** Relative uptake of the **MeF**/**DMeF** mixture (*v*:*v* = 50:50) adsorbed in **BrP6***β* after 24 hours using gas chromatography.

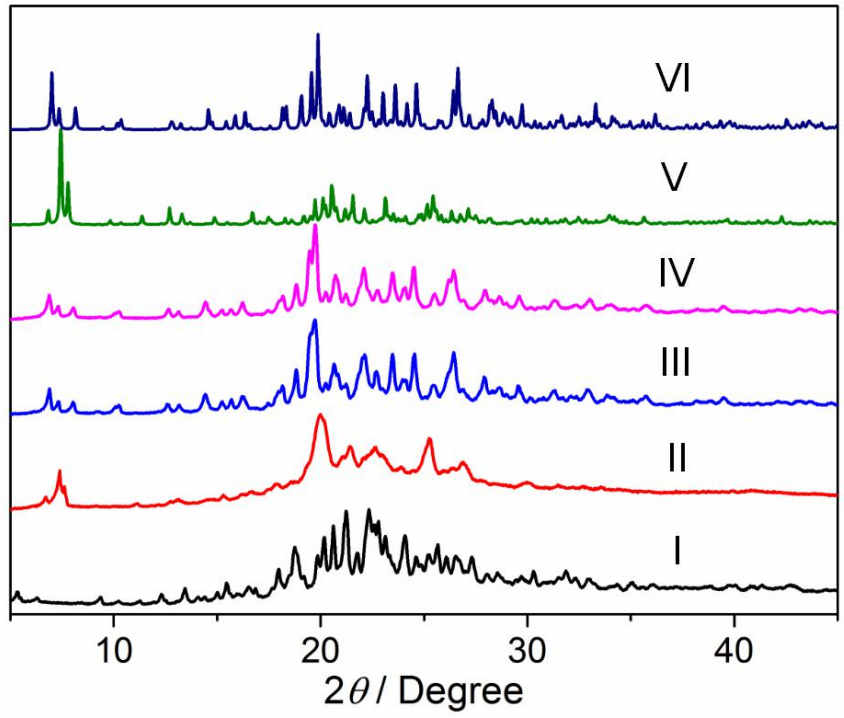


**Figure S63.** Powder X-ray diffraction patterns of **BrP6**: (I) original **BrP6***β*; (II) after adsorption of **MeF** vapor; (III) after adsorption of **DMeF** vapor; (IV) after adsorption of a 50:50 *v*/*v* **MeF** and **DMeF** mixture vapor; (V) simulated from single crystal structure of **(MeF)$_2$@BrP6**; (VI) simulated from single crystal structure of **DMeF@BrP6**.

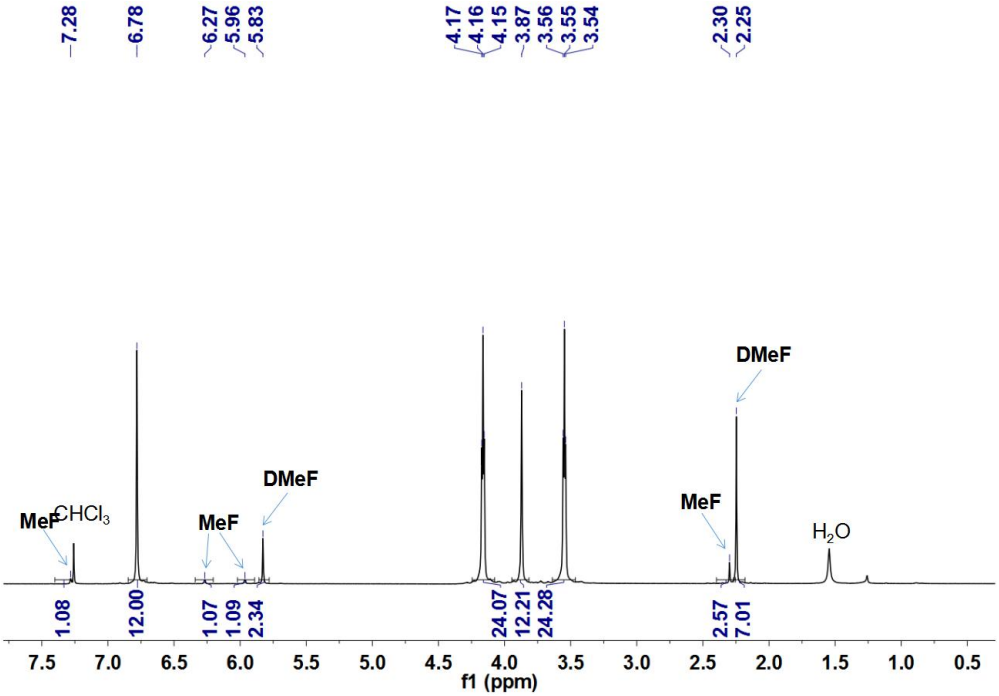


**Figure S64.** [1]H NMR spectrum (600 MHz, chloroform-*d*, 298 K) of **BrP6***β* after adsorption of a 50:50 *v/v* **MeF** and **DMeF** mixture vapor.

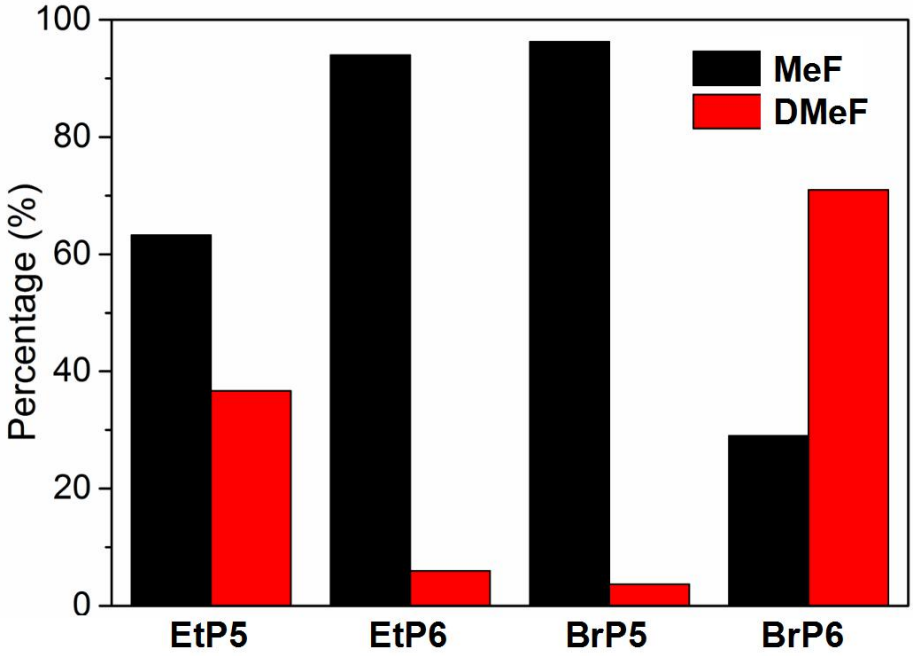


**Figure S65.** Relative uptake of the **MeF**/**DMeF** mixture vapor (*v*/*v* = 50:50) adsorbed in crystals of four pillararenes after 24 hours by GC.

*6. Recyclability of experiments*

*6.1. Recyclability of **EtP6**β crystals*

An open 5.00 mL vial containing 20.00 mg of **(MeF)$_2$@EtP6** was desolvated under vacuum at 60 °C overnight. The resultant crystals were characterized by TGA, PXRD and [1]H NMR.

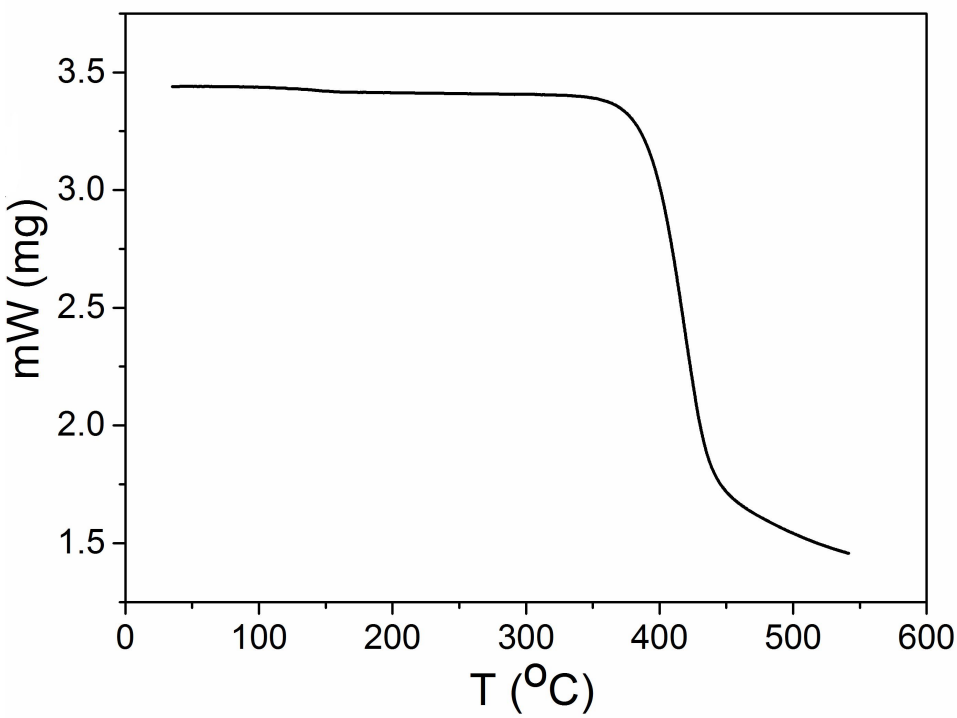


**Figure S66.** Thermogravimetric analysis of desolvated **(MeF)$_2$@EtP6** upon removal of **MeF**.

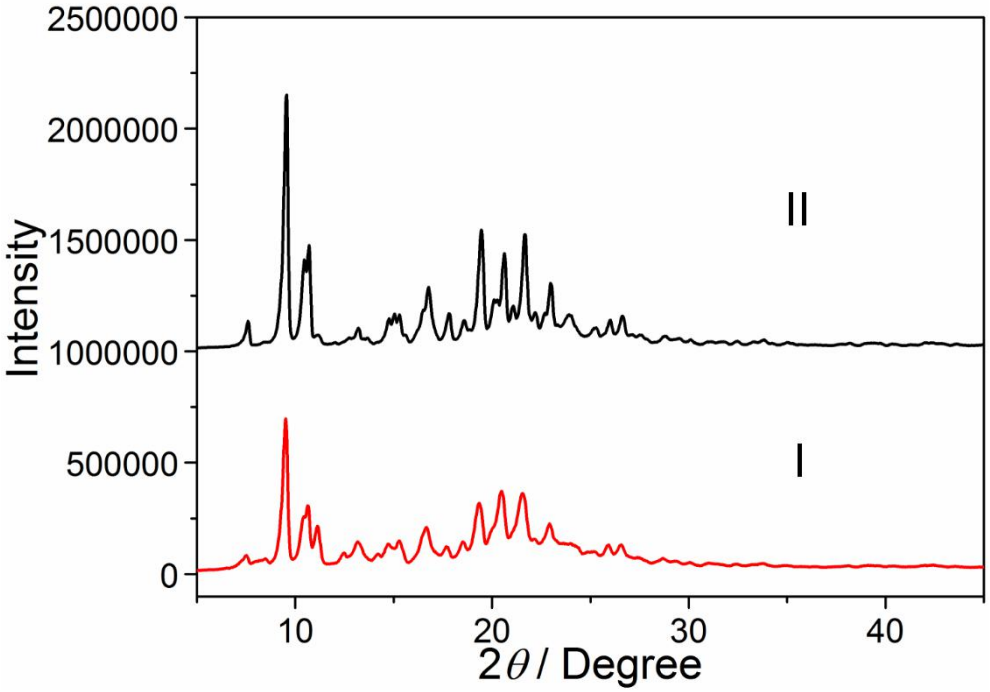


**Figure S67.** Powder X-ray diffraction patterns of **EtP6**: (I) **EtP6**$\beta$; (II) desolvated **(MeF)$_2$@EtP6**. This means that upon removal of **MeF**, **(MeF)$_2$@EtP6** transforms back to **EtP6**$\beta$.

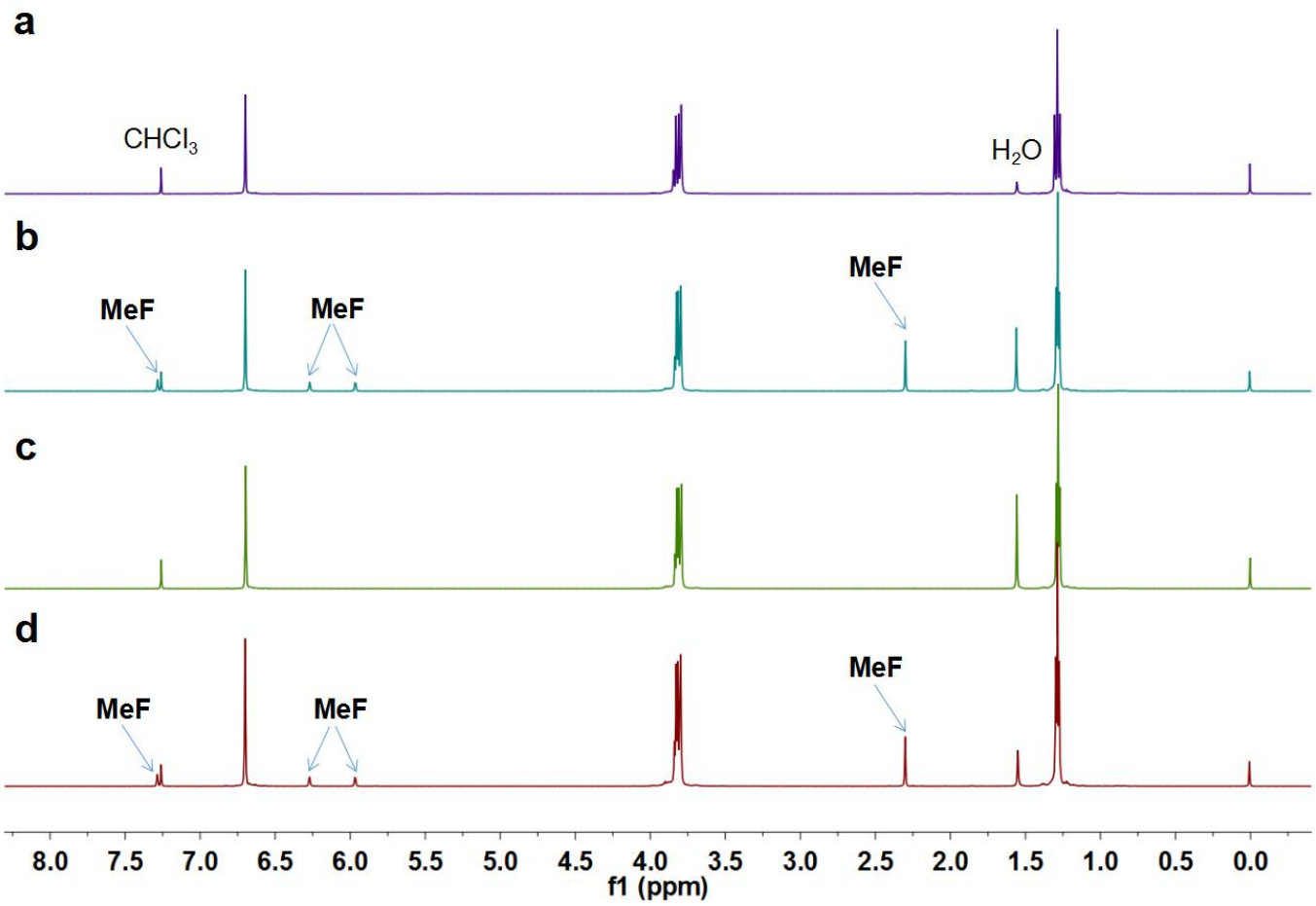


**Figure S68.** $^{1}$H NMR spectra (400 MHz, chloroform-*d*, 298 K): (a) original **EtP6***β*; (b) **EtP6***β* after adsorption of **EtP6** vapor; (c) **(MeF)$_2$@EtP6** after removal of **MeF**; (d) desolvated **(MeF)$_2$@EtP6** after adsorption of **MeF** vapor.

*6.2. Recyclability of **BrP5**α crystals*

An open 5.00 mL vial containing 20.00 mg of **(MeF)$_2$@BrP5** was desolvated under vacuum at 60 ℃ overnight. The resultant crystals were characterized by TGA, PXRD and $^{1}$H NMR.

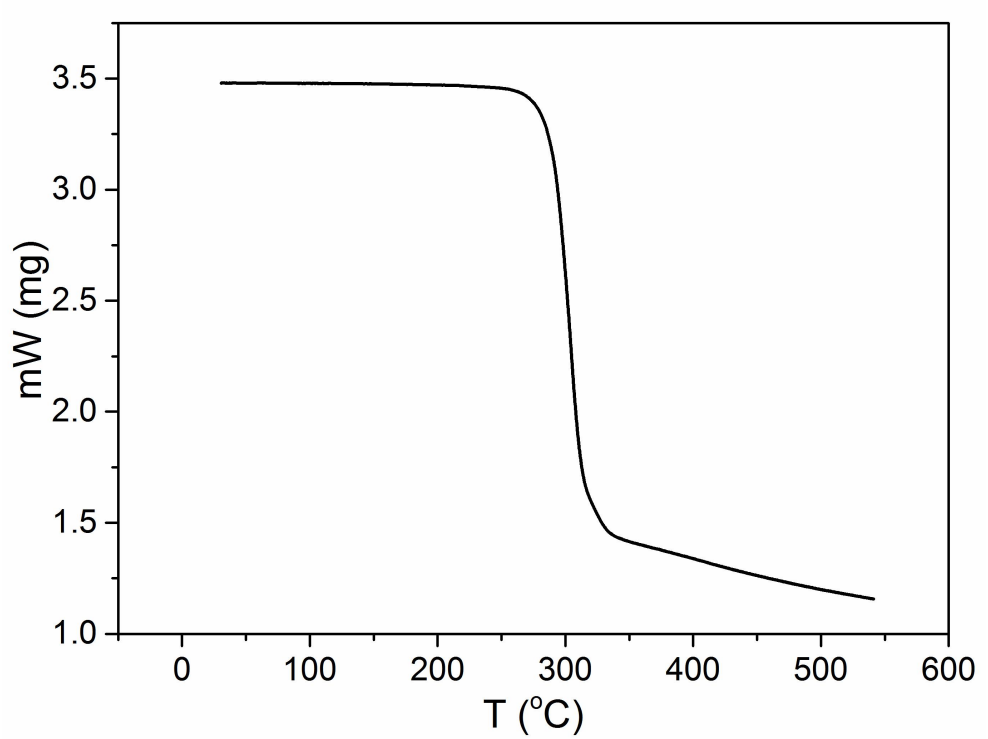


**Figure S69.** Thermogravimetric analysis of desolvated **(MeF)$_2$@BrP5** upon removal of **MeF**.

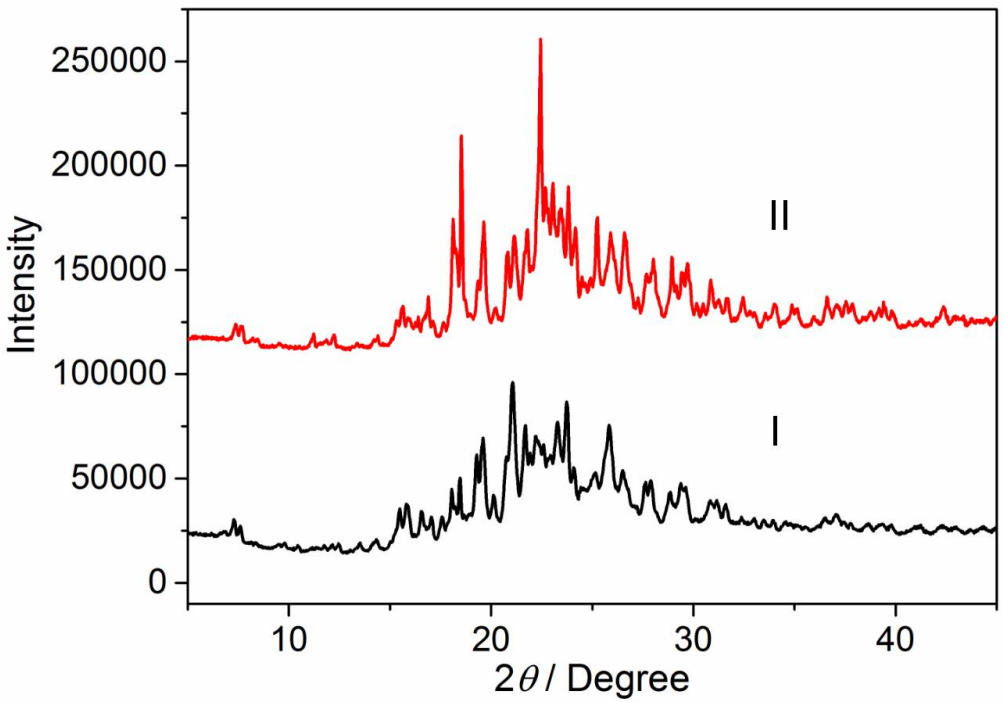


**Figure S70.** Powder X-ray diffraction patterns of **BrP5**: (I) **BrP5**$\alpha$; (II) desolvated **(MeF)$_2$@BrP5**. This means that upon removal of **MeF**, **(MeF)$_2$@BrP5** transforms back to **BrP5**$\alpha$.

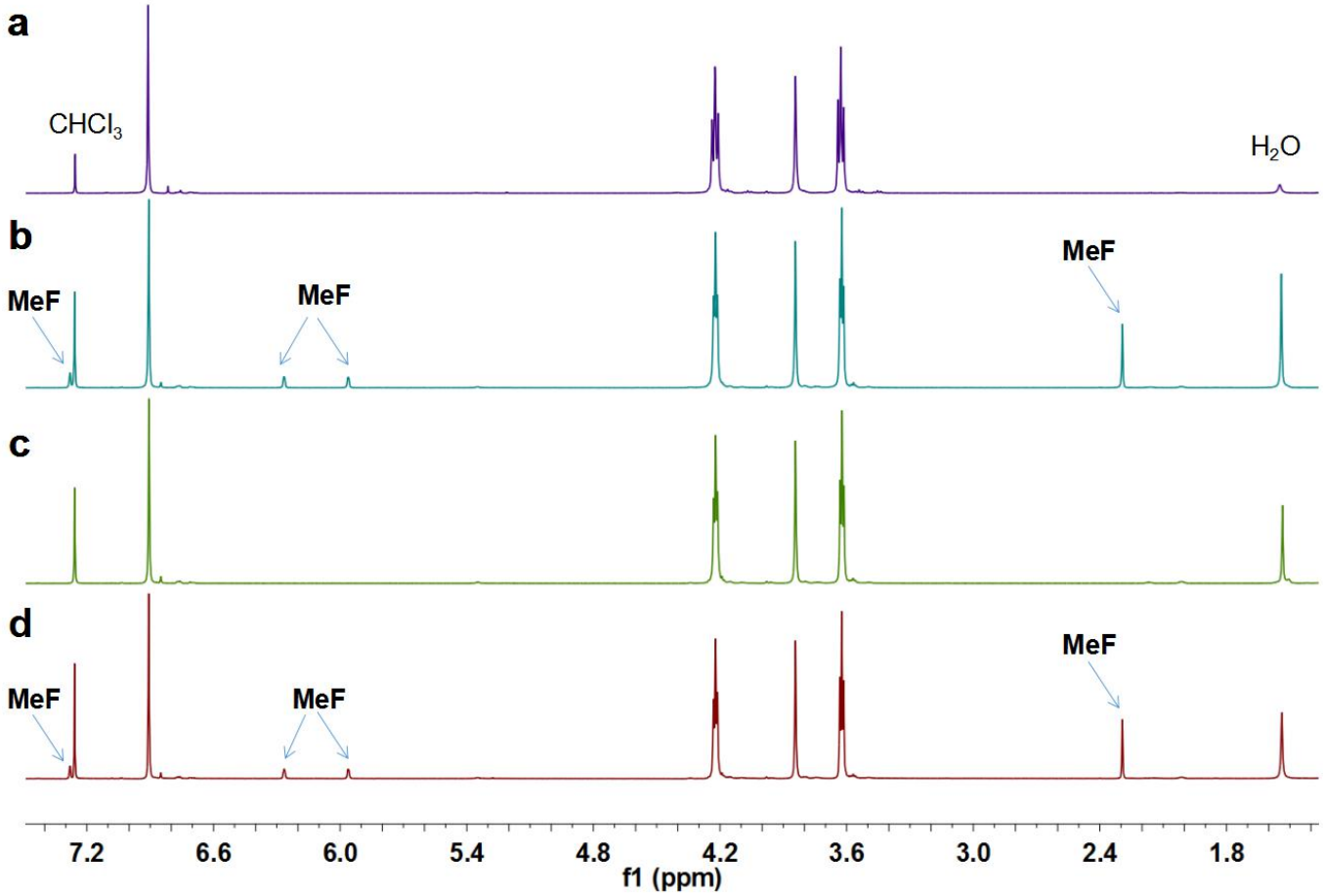


**Figure S71.** $^{1}$H NMR spectra (400 MHz, chloroform-*d*, 298 K): (a) original **BrP5***α*; (b) **BrP5***α* after adsorption of **MeF** vapor; (c) **(MeF)$_2$@BrP5** after removal of **MeF**; (d) desolvated **(MeF)$_2$@BrP5** after adsorption of **MeF** vapor.

*7. Other Vapor-Phase Adsorption cases*

*7.1 Adsorption of 90:10 v/v **MeF** and **DMeF** mixture vapor*

For each vapor-phase mixture experiment, an open 5.00 mL vial containing 20.00 mg of guest-free **EtP6***β* or **BrP5***α* adsorbent was placed in a sealed 20.00 mL vial containing 1.00 mL of a 90:10 *v/v* **MeF** and **DMeF** mixture. The relative uptake of **MeF** or **DMeF** by **EtP6***β* or **BrP5***α* was measured by heating the crystals to release the adsorbed vapor using gas chromatography. Before measurements, the crystals were heated at 60 °C to remove the surface-physically adsorbed vapor.

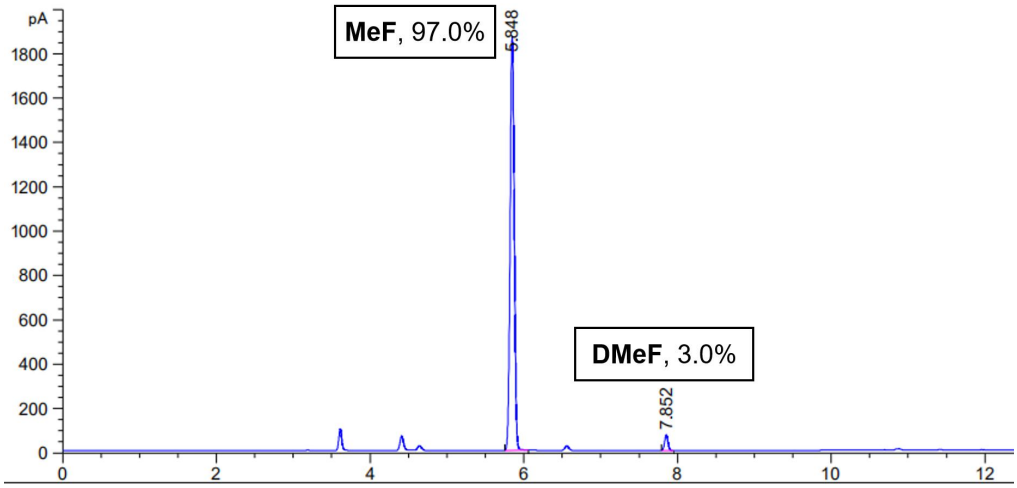


**Figure S72.** Relative uptake of the **MeF**/**DMeF** mixture (*v*:*v* = 90:10) adsorbed in **EtP6***β* after 24 hours using gas chromatography.

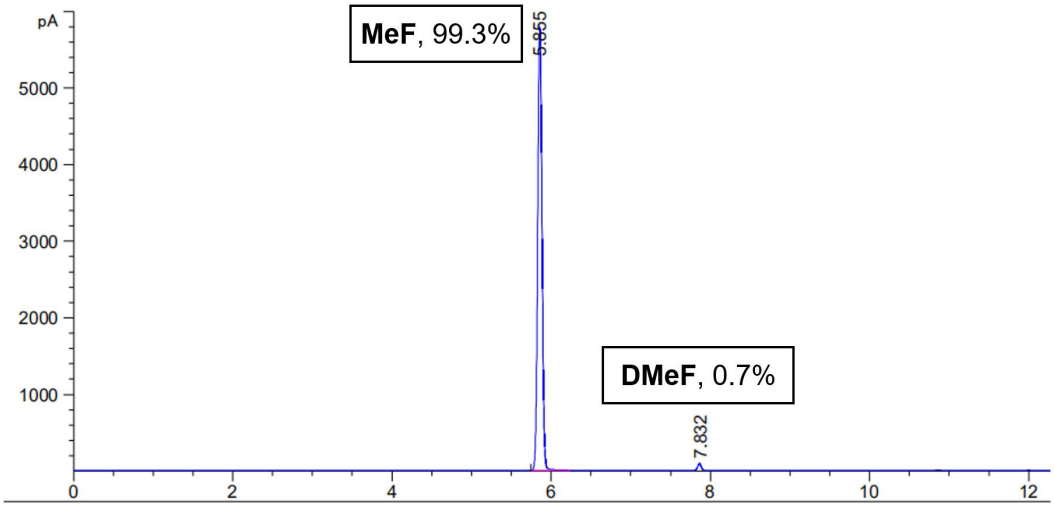


**Figure S73.** Relative uptake of the **MeF**/**DMeF** mixture (*v*:*v* = 90:10) adsorbed in **BrP5***α* after 24 hours using gas chromatography.

*7.2 Adsorption of three component equimolar **MeF**, **DMeF** and **MeTHF** mixture vapor*

For each vapor-phase mixture experiment, an open 5.00 mL vial containing 20.00 mg of guest-free **EtP6***β* or **BrP5***α* adsorbent was placed in a sealed 20.00 mL vial containing 1.00 mL of a 1:1:1 *v/v/v* **MeF**, **DMeF** and **MeTHF** mixture. The relative uptake of **MeF**, **DMeF** or **MeTHF** by **EtP6***β* or **BrP5***α* was measured by heating the crystals to release the adsorbed vapor using gas chromatography. Before measurements, the crystals were heated at 60 ℃ to remove the surface-physically adsorbed vapor.

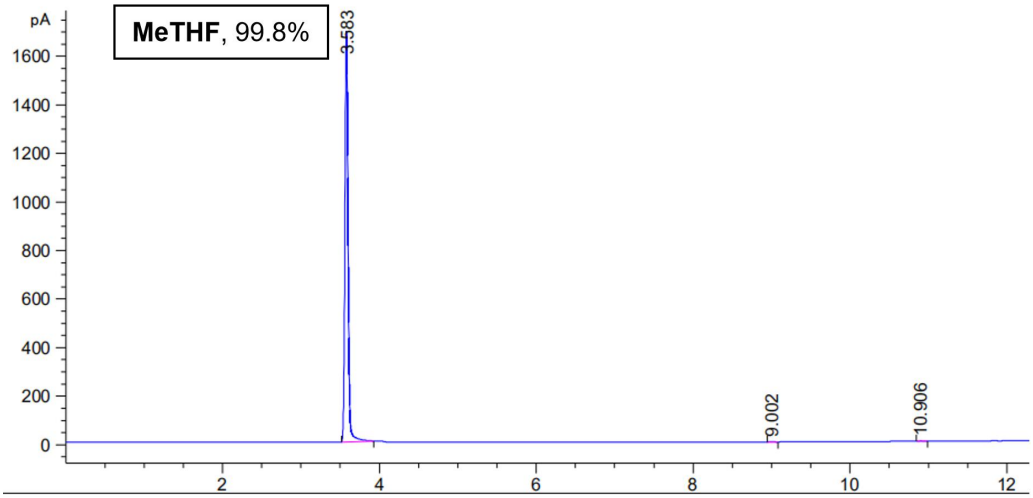


**Figure S74.** GC spectrum of **MeTHF**. This spectrum was obtained to show the position of the **MeTHF** peak.

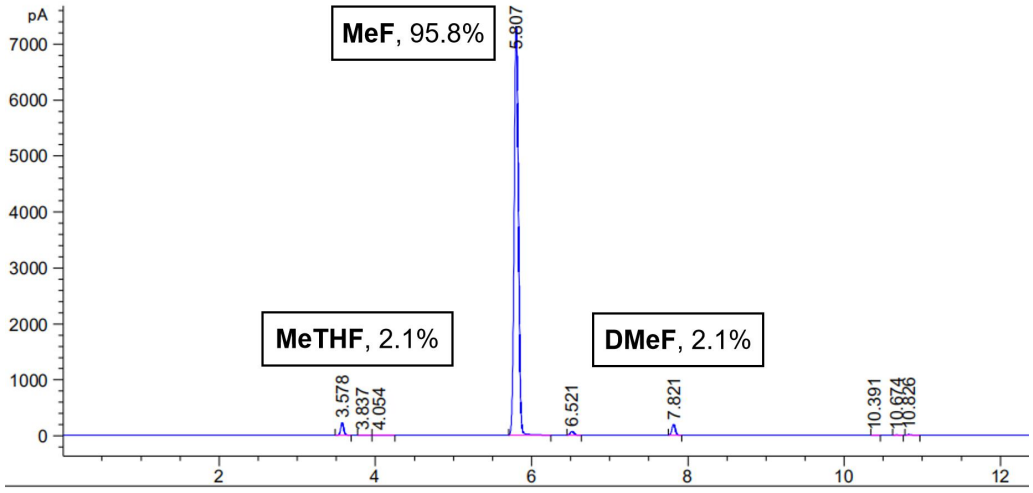


**Figure S75.** Relative uptake of the **MeF**/**DMeF**/**MeTHF** mixture (*v*:*v*:*v* = 1:1:1) adsorbed in **EtP6***β* after 24 hours using gas chromatography.

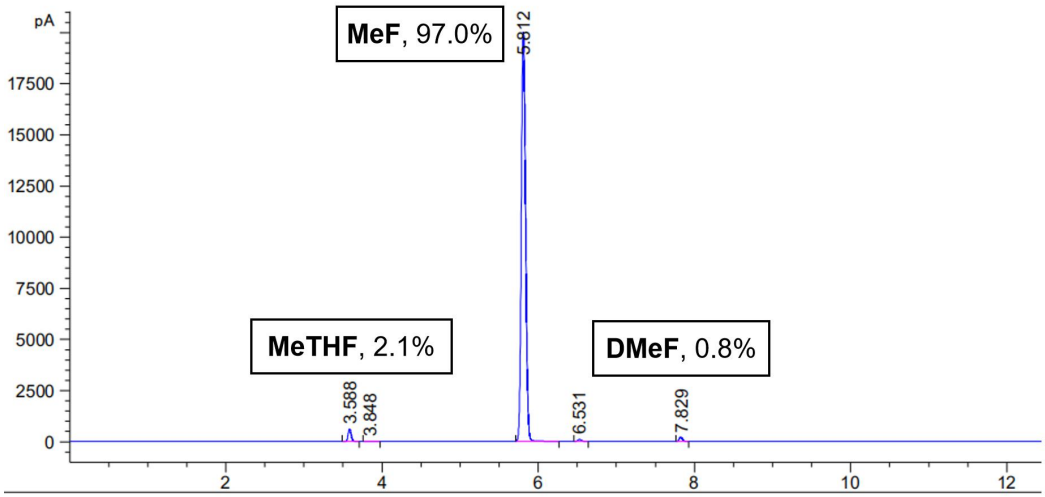

**Figure S76.** Relative uptake of the **MeF/DMeF/MeTHF** mixture (*v*:*v*:*v* = 1:1:1) adsorbed in **BrP5***α* after 24 hours using gas chromatography.

*8. References*

[S1] Hu, X.-B.; Chen, Z.; Chen, L.; Zhang, L.; Hou, J.-L.; Li, Z.-T.; Pillar[*n*]arenes (*n* = 8−10) with Two Cavities: Synthesis, Structures, and Complexing Properties. *Chem*. *Commun*. **2012**, *48*, 10999–11001.

[S2] Yao, Y.; Xue, M.; Chi, X.; Ma, Y.; He, J.; Ablizb, Z.; Huang, F. A New Water-Soluble Pillar[5]arene: Synthesis and Application in The Preparation of Gold Nanoparticles. *Chem*. *Commun*. **2012**, *48*, 6505–6507;

[S3] Yao, Y.; Li, J.; Dai, J.; Chi, X.; Xue, M. A Water-Soluble Pillar[6]arene: Synthesis, Host-Guest Chemistry, Controllable Self-Assembly, and Application in Controlled Release. *RSC Adv*. **2014**, *4*, 9039–9043;

[S4] Jie, K.; Liu, M.; Zhou, Y.; Little, M. A.; Pulido, A.; Chong, S. Y.; Stephenson, A.; Hughes, A. R.; Sakakibara, F.; Ogoshi, T.; Blanc, F.; Day, G. M.; Huang, F.; A. I. Cooper, Near-Ideal Xylene Selectivity in Adaptive Molecular Pillar[n]arene Crystals. *J. Am. Chem. Soc.* **2018**, *140*, 6921−6930;

[S5] Lide, D. R. CRC Handbook of Chemistry and Physics, Boca Raton, FL, **2005**, pp. 203–365.